博士論文

Functional analysis of the replication factor, Mcm10, in the initiation of chromosomal DNA replication in *Saccharomyces cerevisiae*

（出芽酵母の染色体 DNA 複製開始反応における Mcm10 の機能解析）

Joji (George) Watase

Department of Biological Sciences
Graduate School of Science
Osaka University

Contents

Abstract

Chromosomal DNA replication in eukaryotes is initiated at multiple sites called replication origins where conserved replication factors work for the initiation of DNA replication. A key process in the initiation is to convert the inactive Mcm2-7 helicase to the active Cdc45-Mcm2-7-GINS (CMG) helicase complex. Replication forks are established after CMG formation. However, it is still poorly understood the mechanism involved in fork establishment yet. Mcm10 is a conserved protein essential for the initiation and its reported functions have been controversial. It is, therefore, important to define the role of Mcm10 in order to understand the molecular mechanism of the initiation. To characterize the role of Mcm10, I generated a novel conditional allele of *mcm10* in budding yeast by combining the recently developed auxin-inducible degron (AID) system with the *mcm10-1* temperature-sensitive (ts) mutation. The resultant *mcm10-1-aid* strain, in which Mcm10 can be efficiently depleted in response to auxin, showed a strong defect in the initiation of replication. In the absence of Mcm10, a stable CMG complex was assembled at origins. However, subsequent translocation of CMG and origin unwinding were severely diminished. These results strongly suggest that there is a novel step for activating assembled CMG in the presence of Mcm10. Furthermore, I found that, among the CMG components, Mcm10 strongly interacts with Mcm2 and Mcm6. Taken together with the fact that Mcm10 has DNA binding activity, I propose that Mcm10 plays an essential role in the conformational change of Mcm2-7 for CMG activation.

Introduction

I. DNA replication is initiated at replication origins

Chromosomal DNA replication is initiated at specialized loci called replication origins (Figure 1, G1). In eukaryotes, multiple replication origins are distributed on individual chromosomes. All replication origins have been identified in budding and fission yeasts (Hayashi et al., 2007; Raghuraman et al., 2001). Recent genome-wide studies of human, mouse, and *Drosophila* showed that replication origins are enriched in proximity to active transcription start sites (Cayrou et al., 2010; Dellino et al., 2013; Mechali, 2010). Furthermore, it has been reported that there is a correlation exists between replication origin loci and CpG islands (Cadoret et al., 2008; Cayrou et al., 2010; Delgado et al., 1998; Gomez and Antequera, 2008; Sequeira-Mendes et al., 2009). Taken together with the fact that CpG islands control gene transcription activity, it has been proposed that CpG islands are landmark of replication origins in these species. However, distinct short stretch of origin sequences such as found in yeasts have not been identified in these species.

Two cell-cycle dependent kinases, Dbf4-dependent kinase (DDK) and Cyclin-dependent kinase (CDK), are involved in the activation of origins. Importantly, origins are not activated at once in S phase; some are activated in early S phase (early origins; Figure 1, Early S), and others in late S phase (late origins; Figure 1, Late S). Furthermore, there is origins that are not activated in normal S phase (dormant origins). Bi-directional replication forks are

established at activated origins with subsequent translocation of forks moving away from the origins (Figure 1, Early or Late S). After convergence of replication forks, whole chromosomal DNA is replicated (Figure 1, G2).

II. Pre-RC formation and its activation

Many replication factors that associate with replication origins are involved in the initiation of replication. The hetero-hexameric origin recognition complex (ORC), composed of the Orc1-6 subunits, associates with origins through the cell cycle (Figure 2a). ORC is an ATPase and its binding to origin DNA requires ATP-hydrolysis (Bell and Stillman, 1992; Klemm et al., 1997; Lee et al., 2000; Speck et al., 2005; Takenaka et al., 2004). Previous studies using yeast and *Xenopus* egg extracts showed that origin-bound ORC recruits the ATPase Cdc6, and a coiled-coil protein, Cdt1, to origins from late M to G1 phase. Subsequently, the hexameric-replicative helicase, Mcm2-7, is loaded onto replication origins to form the pre-replicative complex (pre-RC; Figure 2b) (Masai et al., 2010). Recently, a pre-RC reconstitution experiment using purified yeast proteins showed that ORC, Cdc6, and Cdt1 are essential and sufficient to load Mcm2-7 onto origin DNA (Evrin et al., 2009; Remus et al., 2009). Furthermore, it has been reported that ATP hydrolysis by ORC-Cdc6 is essential for the stable association of Mcm2-7 double hexamer with origins in the presence of Cdt1 (Frigola et al., 2013). Importantly, Mcm2-7 in pre-RC is not active as a replicative helicase and thus replication is not initiated in G1 phase.

To activate pre-RC, activation of DDK and CDK is necessary. Genetic and biochemical analyses with yeast and *Xenopus* egg extracts have contributed to the identification of essential factors involved in pre-RC activation. DDK, which is activated from late G1 to early S phase, phosphorylates Mcm2-7 (Figure 2c) (Sheu and Stillman, 2006, 2010). This phosphorylation allows initial association of Sld3 (Treslin/Ticrr in metazoans) and Cdc45 with Mcm2-7 (Figure 2c) (Heller et al., 2011; Kamimura et al., 2001b; Kanemaki and Labib, 2006; Tanaka et al., 2011; Yabuuchi et al., 2006). Subsequently, S-CDK phosphorylates Sld2 and Sld3 in S phase (Figure 2d) (Tanaka et al., 2007; Zegerman and Diffley, 2007). S-CDK activation also promotes formation of another complex called the pre-loading complex (pre-LC), which contains phosphorylated Sld2, DNA polymerase ε (Polε), tetrameric GINS complex, and Dpb11 (TopBP1 in metazoans) in budding yeast (Muramatsu et al., 2010). Dpb11 has BRCT repeats, which bind phospho-Sld3 and phospho-Sld2 through its N- and C-termini, respectively. Therefore, Cdc45, GINS, and Mcm2-7 assemble at pre-RC to form the Cdc45-Mcm2-7-GINS (CMG) complex (Figure 2e). Once CMG is formed, Mcm2-7 is activated for unwinding of double-stranded DNA (dsDNA) at origins. After origin unwinding, replication protein A (RPA), a single-stranded DNA (ssDNA) binding protein, binds to exposed ssDNA. DNA polymerase α (Polα) comprises primase synthesizes DNA after priming short RNA (Figure 2f). Subsequently, DNA polymerase δ (Polδ) or Polε extends the RNA-DNA fragments synthesized by Polα (Figure 2g). In the current model, Polδ and

Polε synthesize leading- and lagging- strands, respectively (Nick McElhinny et al., 2008; Pursell et al., 2007). A large replication machinery complex called the replisome is formed at origins before translocation of forks. Sld2, Sld3, and Dpb11 are not found in replisome, suggesting they are required only for the initiation.

III. Mcm2-7 is the key factor in the replication control

Mcm2-7 was first identified in a genetic screen for plasmid-loss mutants in budding yeast (Maine et al., 1984). Later, biochemical analyses with *Xenopus* egg extracts showed that Mcm2-7 is the licensing factor that permits cells to replicate their chromosomal DNA only once per cell cycle (Chong et al., 1995; Kubota et al., 1995). Like other replicative DNA helicases, such as Simian Virus 40 (SV40) T-antigen and prokaryotic DnaB, Mcm2-7 forms a ring-shaped hexameric complex, composed of evolutionarily related AAA+ ATPase subunits containing a conserved MCM domain (Bochman and Schwacha, 2009). Although the Mcm2-7 sub-complex, Mcm4-6-7, shows helicase activity *in vitro* (Bochman and Schwacha, 2009; Ishimi, 1997; Kaplan et al., 2003; Lee and Hurwitz, 2000), biochemically purified Mcm2-7 does not show robust helicase activity unless under a specific anionic condition (Bochman and Schwacha, 2009). Interestingly, the CMG complex has 3' to 5' helicase activity *in vitro* (Ilves et al., 2010; Moyer et al., 2006), and is a part of replisome (Calzada et al., 2005; Gambus et al., 2006; Pacek et al., 2006). Therefore, it is thought that CMG is the bona fide replicative helicase. These

biochemical analyses are consistent with the idea that Mcm2-7 in pre-RC is not active as helicase and is converted to the active form by CMG formation in S phase.

Several evidence suggested that Mcm2-7 in pre-RC forms a head-to-head double-hexameric complex (Evrin et al., 2009; Gambus et al., 2011; Remus et al., 2009). In contrast, it has been shown that Mcm2-7 works as a single hexamer in the replisome (Gambus et al., 2006; Yardimci et al., 2010). Therefore, it has been suggested that the Mcm2-7 double-hexamer dissociates during the initiation of replication. Furthermore, it has been shown that Mcm2-7 in pre-RC encircles dsDNA (Evrin et al., 2009; Remus et al., 2009). In contrast, a recent report suggested that Mcm2-7 in the replisome encircles ssDNA on the leading strand (Fu et al., 2011). Therefore, it is likely that Mcm2-7 initially encircles dsDNA and then converts to encircle ssDNA at the time when CMG is activated during initiation. Even though many replication factors involved in pre-RC or CMG formation have been identified, the mechanism involved in the dissociation and structural conversion of Mcm2-7 remains elusive.

IV. Mcm10 is an essential replication factor conserved in all eukaryotes

Mcm10 is an essential and conserved protein in all eukaryotes. It was originally identified by two independent genetic screens for temperature sensitive (ts) mutations affecting DNA replication and for plasmid-loss

mutations (Dumas et al., 1982; Maine et al., 1984; Merchant et al., 1997; Solomon et al., 1992). The latter screening also identified Mcm2-7. It has been reported that Mcm10 interacts with many replication factors, such as ORC, Mcm2-7, Cdc45, Dpb11, Polε and Polα (Homesley et al., 2000; Kawasaki et al., 2000; Merchant et al., 1997; Ricke and Bielinsky, 2006). Furthermore, previous studies using yeast *mcm10* ts mutants showed that Mcm10 plays an essential role in the initiation (Homesley et al., 2000; Merchant et al., 1997). The conserved central region of Mcm10 includes the OB-fold/Zn-finger domain, which contains clusters of basic residues forming a ssDNA-binding domain (Warren et al., 2008). In fact, *in vitro* studies showed that Mcm10 binds to both ssDNA and dsDNA (Eisenberg et al., 2009; Fien et al., 2004; Robertson et al., 2008; Warren et al., 2009; Warren et al., 2008). However, the essential role of Mcm10 in the initiation remains controversial (Table 1). Previous studies with *Xenopus* egg extracts and with budding and fission yeasts showed that Mcm10 is required for Cdc45 loading (Gregan et al., 2003; Sawyer et al., 2004; Wohlschlegel et al., 2002). In contrast, other studies in budding yeast and human cells reported that Mcm10 is required for stability of Polα (Chattopadhyay and Bielinsky, 2007; Ricke and Bielinsky, 2004). The latter study also suggested that Mcm10 is regulated for the elongation of replication fork, because Polα is required for the lagging strand synthesis. However, another report in human cells showed that Polα stability is not affected even when Mcm10 is depleted by siRNA (Zhu et al., 2007). A recent *in vitro* reconstitution experiment using budding yeast extract does not

support these previous findings, but showed that Mcm10 plays a role after loading of Cdc45 and GINS (Heller et al., 2011). Therefore, it is important to define the role of Mcm10 for understanding of the molecular mechanism of the initiation. In this study, I aimed to characterize the role of Mcm10 in the initiation.

V. In this study

Budding yeast is an ideal model organism for understanding the mechanism of the initiation of replication for following reasons. First, the loci of all replication origins on chromosomes and the timing of their initiation are well known (Raghuraman et al., 2001). Second, it is possible to synchronize cells in G1 phase, just before the initiation, using mating pheromones called the a/α factor; this enables us synchronous analysis of the initiation reaction by releasing the cells from G1 block. Third, the frequency of homologous recombination (HR) is high, enabling mutant generation by engineering endogenous genes. Because Mcm10 is conserved in all eukaryotes, I used budding yeast as a model organism to study the role of Mcm10. The *mcm10* ts mutants have been widely used to study the role of Mcm10 in budding yeast (Homesley et al., 2000; Merchant et al., 1997; Sawyer et al., 2004). However, characterizing the role of Mcm10 through these conventional mutants has been rather difficult because of a leaky phenotype. To overcome this problem, I generated a tight *mcm10* conditional mutant, *mcm10-1-aid*, by combining recently developed auxin inducible degron (AID) system with *mcm10-1* ts allele

(Figure 3) (Nishimura et al., 2009). Using the *mcm10-1-aid* strain, I revealed that Mcm10 plays a role in a time window following CMG formation and preceding origin unwinding, but is neither required for Cdc45 loading nor Polα stability unlike previously reported (Ricke and Bielinsky, 2004). Furthermore, I found that, among CMG components, Mcm10 strongly interacts with Mcm2 and Mcm6. These observations are consistent with the idea that Mcm10 plays a role in the conformational change of Mcm2-7 necessary for the conformation of CMG.

Materials and methods

Saccharomyces cerevisiae strain

For the carboxy terminus tagging of Mcm10 and Mcm10-1 with the aid degron, the aid-*KanMX* sequence was amplified from pMK43 using primers #42 and #43. All primer sequences used in the present study are summarized in Table 3. The PCR product was transformed into W303-1a and BTY100 (*mcm10-1*), respectively. The resultant strains, YJW18 (*mcm10-aid*) and YJW19 (*mcm10-1-aid*), were confirmed by genomic PCR using following primer sets, #44 and #45, #44 and #47, and #46 and #45. Expression of Mcm10-aid and Mcm10-1-aid proteins were confirmed by western blotting using aid polyclonal antibody. For fusing 5FLAG (5 copies of FLAG) epitope tag to the carboxy terminus of Mcm10, the 5FLAG-*HIS3MX* sequence was amplified from pKL259 using primers #42 and #43. The PCR product was

transformed into W303-1 diploid strain. The resultant strain was confirmed by genomic PCR using following sets of primers, #44 and #45, #44 and #49, and #48 and #45. Expression of Mcm10-5FLAG protein was checked by western blotting using M2 FLAG monoclonal antibody. YJW30 haploid cells (*MCM10-5FLAG*) were derived from tetrad analysis. To generate cells expressing Rfa1-5FLAG or Pol1-5FLAG, the 5FLAG-*HIS3MX* sequence was amplified from pKL259 using primers #50 and #51 or #54 and #55, respectively. Each PCR product was transformed into YNK43 (*MAT*α *GAL-OsTIR1)*. The resultant strains, YJW90 (*MAT*α *RFA1-5FLAG, GAL-OsTIR1*) and YJW64 (*MAT*α *POL1-5FLAG, GAL-OsTIR1*) were confirmed by genomic PCR using following primer sets, #52 and #53, #52 and #49, #48 and #53 (for Rfa1-5FLAG), and #56 and #57, #56 and #49, #48 and #57 (for Pol1-5FLAG), respectively. Expression of Rfa1-5FLAG and Pol1-5FLAG proteins was confirmed by western blotting using M2 FLAG monoclonal antibody. For generating YJW156 diploid cells (*MCM10/Δmcm10*), *hphNT* cassette was amplified from pYM20 using a set of primer, #58 and #43. The PCR product was transformed into W303-1 diploid cells. The replacement of one-allele *MCM10* ORF to *hphNT* cassette was confirmed by genomic PCR using following primer sets, #59 and #45, #59 and #61, and #60 and #45. All yeast strains used in this study are listed in Table 2.

Culture of budding yeast

Medium used in this study except for plasmid shuffle and yeast two-hybrid

assays was YP medium (1 % yeast extract [BD], 2 % peptone [Oxoid]) supplemented with 2 % of glucose (YPD), raffinose (YPR) or galactose (YPG). For growing the cells used for plasmid shuffle assay and yeast two-hybrid assay, SC medium (1xYeast Nitrogen Base, 2% of glucose, 0.14% of Yeast Synthetic Drop-out Medium Supplements [Sigma]) or SD medium (1xYeast Nitrogen Base, 2% of glucose) was used. Detail information is described in materials and methods for Plasmid shuffle assay and Yeast two-hybrid assay, respectively. To induce degradation of aid tagged proteins, exponentially growing cells in YPR at 24˚C were transferred to YPG to induce the expression of OsTIR1-9Myc for 50 min at 24˚C. A natural auxin, indole-3-acetic acid (IAA) (Wako), was then added to medium at a final concentration of 500 μM. Detailed conditions are described in the figure legends.

Protein detection

Protein extracts from budding yeast cells was processed by TCA extraction. Protein samples were separated by SDS-PAGE and transferred to Amersham Hybond-ECL nitrocellulose membrane (GE healthcare) using semi-dry blotter machine. 5% skimmed milk was used as blocking reagent, except for blotting a membrane using Mcm10 polyclonal antibody (2% ECL advance blocking reagent was used) and GFP polyclonal antibody (10% skimmed milk was used). To detect the protein, I used following primary antibodies in this study; anti-Mcm10 polyclonal antibody (Gifted from H. Araki; 1:10000 in 2% ECL advance blocking reagent), anti-aid monoclonal antibody (1:500 in 5%

skimmed milk), 12CA5 anti-HA monoclonal antibody (Roche; 1:2000 in 5% skimmed milk), anti-Ctf4 polyclonal antibody (Gifted from K. Labib; 1:1000 in 5% skimmed milk), M2 anti-FLAG monoclonal antibody (Sigma; 1:2000 in 5% skimmed milk), anti-Mcm4 polyclonal antibody (yC-19, Santa Cruz Biotechnology; 1:200 in 5% skimmed milk), anti-Rad53 polyclonal antibody (yC-19, Santa Cruz Biotechnology; 1:1000 in 5% skimmed milk), anti-Pol1 polyclonal antibody (Gifted from K. Labib; 1:1000 in 5% skimmed milk), 6D2 anti-Pol12 monoclonal antibody (Gifted from M. Foiani and S. Mimura; 1:1000 in 5% skimmed milk), and anti-GFP (code No. 598, MBL; 1:1000 in 1% skimmed milk). Following secondary antibodies used in this study; Donkey anti-rabbit IgG-HRP (GE healthcare; for anti-Mcm10- and anti-GFP- blotting), horse anti-mouse IgG-HRP (Vector laboratories; for anti-aid-, anti-HA-, anti-FLAG-, and anti-Pol12- blotting), donkey anti-sheep IgG-HRP (Sigma; for anti-Ctf4- and anti-Pol1- blotting), and donkey anti-goat IgG-HRP (Santa Cruz Biotechnology; for anti-Mcm4- and anti-Rad53- blotting). All of secondary antibodies were diluted to 1:5000 using same solutions used for each primary antibody. To detect the signal of target proteins, following detection reagents was used; ECL (GE healthcare; for anti-HA, anti-FLAG-, and for anti-Pol1-blotting), ECL prime (GE healthcare; for anti-aid-, anti-Ctf4-, anti-Mcm4-, anti-Rad53-, anti-Pol12-, and anti-GFP- blotting), and ECL advance (GE healthcare: for anti-Mcm10 blotting). All of the images were taken by an ImageQuant LAS4000 mini system (GE Healthcare)

Quantification of Mcm10 depletion efficiency

Band intensity of Mcm10 and Mcm10-1-aid were measured using Multi Gauge software (FUJIFILM). I surrounded each Mcm10 and Mcm10-1-aid band by same-pixel sized square (2542 $pixel^2$) and measured their intensity with subtracting background intensity. Detail information is described in Figure S1.

Flow cytometry

Cells were fixed in 70 % EtOH. After processing with 0.1mg/ml RNase A for 2 hours at 37^{o}C and then 5mg/ml pepsin for 30 minutes at 37^{o}C, cells were stained with 2 μg/ml propidium iodide. Propidium iodide stained cells were analyzed using a FACSCalibur system (BD).

Chromatin immunoprecipitation (ChIP) assay

Cells (1.75 x 10^8) were collected and cross-linked with 1% formaldehyde for 20min, then mixed with 120 mM Glycine for 5 min to stop cross-linking reaction. Cells were briefly washed with ice cold TBS and Lysis buffer (50 mM HEPES-KOH pH7.5, 140 mM NaCl, 1% Triton X-100, 0.1% Sodium deoxycholate, 20 mM β-glycerophosphate, 50 mM NaF, 0.1 mM Na_3VO_4, 0.5 mM sodium pyrophosphate, 1 mM EDTA), then mixed with Lysis working solution (added 1 mM PMSF, 1 x Complete EDTA-free protease inhibitor (Roche) to Lysis buffer) and vortexing with glass beads in a Multi-beads shocker (Yasui kikai) at 4^{o}C. Genomic DNA was fragmented by sonication

(Model 250, Branson) before immunoprecipitation using magnetic beads (Dynabeads protein G, Veritas) conjugated with anti-FLAG (M2, Sigma) or anti-Myc (9E11, Santa Cruz) monoclonal antibody. After immunoprecipitation, samples were washed twice each with following three different buffers. Buffer1 (50 mM HEPES-KOH pH7.5, 140 mM NaCl, 1% Triton X-100, 0.1% Sodium deoxycholate, 20 mM β-glycerophosphate, 50 mM NaF, 0.1 mM Na_3VO_4, 0.5 mM sodium pyrophosphate, 1 mM EDTA), buffer2 (50 mM HEPES-KOH pH7.5, 500 mM NaCl, 1% Triton X-100, 0.1% Sodium deoxycholate, 20 mM, 1 mM EDTA) and buffer3 (10 mM Tris-HCl pH8.0, 250 mM LiCl, 0.5% NP-40, 0.5% Sodium deoxycholate, 1 mM EDTA). I incubated the immunoprecipitated samples at 65˚C for 10min with elution buffer (50 mM Tris-HCl pH8.0, 10 mM EDTA, 1% SDS). In the case of Rfa1-5FLAG ChIP, immunoprecipitates were extensively washed in a wash buffer containing 0.025 % SDS to strip non-specific DNA bound to Rfa1 during IP. After purification of associated DNA fragments, we used a quantitative PCR instrument (Chromo4, Bio-Rad) to calculate the enrichment of particular sequences in the chromosomes. PCR primers used and the location of detected sequences on the chromosomes are given in Table 2. PCR reactions were set using the Thunderbird SYBER qPCR mix (Toyobo) and the data were analyzed using the Opticon Monitor software (Bio-Rad) to obtain Ct values. Enrichment in IP samples relative to input DNA was calculated using the following equation. IP recovery (%) = $2^{Ct(input)}/2^{Ct(IP)}$. In Figure 10 b and c, the obtained IP recovery of the indicated locus at each time point was

normalized relative to that of the + 6kb locus at 0 min for the comparison of two ChIP data sets (ChIP for Cdc45-18Myc and Mcm10-5FLAG). I performed three PCR reactions for each ChIP sample to obtain an SD. All ChIP data were confirmed by independent two experiments. The ChIP results derived from independent experiments are shown in Figure S2-S5.

Immunoprecipitation assay

Cells (1.75×10^8) were collected and lysed in 0.4 ml of IP buffer (50 mM HEPES-KOH pH7.5, 150 mM KOAc, 1 % Triton X-100, 20 mM β-glycerophosphate, 50 mM NaF, 0.1 mM Na_3VO_4, 0.5 mM sodium pyrophosphate, 1 mM EDTA, 1 mM PMSF, 1 x PhosSTOP phosphatase inhibitor (Roche), 1 x Complete EDTA-free protease inhibitor (Roche), 1 x protease inhibitor cocktail (P8215, Sigma) by vortexing with glass beads in a Multi-beads shocker (Yasui kikai) at 4°C. Crude extracts were treated with 125 U of benzonase nuclease (Novagen) for 30 min on ice to digest DNA. After centrifugation to remove insoluble materials, the clear supernatants were mixed with anti-FLAG conjugated agarose (M2 agarose, Sigma) for 2 h at 4°C. The beads were washed with IP buffer containing the indicated concentration of KOAc or NaCl. Bound proteins were eluted with SDS-sample buffer.

Plasmid shuffle assay

To generate haploid *Δmcm10* cells, pJW3 (pRS316/*MCM10*) was transformed into YJW156 diploid cells (*MCM10/Δmcm10*) by non-integrative transformation

followed by sporulation and selection for *MATa*, -Ura (pJW3) and Hygromycin (*Δmcm10*) resistance. In pJW3, to express *MCM10* under native *MCM10* promoter, *MCM10* ORF and its 500 bp 5' UTR and 300 bp 3' UTR regions were amplified from W303-1a genomic DNA using following primer sets, #62 and #63. The PCR product was inserted into pRS316 at EcoRI and XmaI site. Amplified region was checked by DNA sequencing. To express GFP-NLS fusing full length or the amino- or carboxy- terminus deletion mutants of Mcm10 from native *MCM10* promoter, GFP-NLS sequence was derived from pNHK12 and inserted into pRS414 at ApaI and KpnI sites (pJW4). Native *MCM10* promoter region was amplified from pJW3 using primers, #64 and #65. The PCR product was inserted into pJW4 at EcoRI and ApaI sites (pJW5). Amplified region was confirmed by DNA sequencing. Full length of Mcm10, the amino- (Mcm10ΔN150 [amino acid: 151-571]) or carboxy- (Mcm10ΔC107 [amino acid: 1-465] and Mcm10ΔC60 [amino acid: 1-512]) terminus deleted Mcm10 were obtained by PCR from pJW3 using following primer sets, #15 and #18, (full length), #16 and #18 (ΔN150), #15 and #17 (ΔC107), and #15 and #19 (ΔC60), respectively. Amplified regions were confirmed by DNA sequencing. The PCR products were cloned into pJW5 at ApaI site (pJW6 [pRS414/*MCM10*], pJW7 [pRS414/*mcm10ΔN150*], pJW8 [pRS414/*mcm10ΔC107*], and pJW12 [pRS414/*mcm10ΔC60*]). pJW6, pJW7, pJW8, and pJW12 were transformed into YJW158 cells (*Δmcm10*, pRS316/*MCM10*) and selected on SD-Leu-Ura plates. The transformants were isolated and grown in SC media overnight, and 10-fold serial dilutions

starting from $5.0x10^4$ cells were spotted onto either SC-Trp or SC-Trp+5-FOA (final concentration is 0.1% [w/v]) plates to select for loss of pJW3 (pRS316/*URA3*) carrying the wild type *MCM10*. Spotted cells were grown at 30˚C for 2-4 days. The primers and plasmids used in this assay are shown in Table 3 and 4, respectively.

Yeast two-hybrid assay

The constructs of Mcm10ΔC60 (amino acid: 1-512), the amino terminus portion of Mcm10 (amino acid: 1-150), central region of Mcm10 (amino acid: 151-370), and the carboxy terminus of Mcm10 (amino acid: 371-571) were amplified from pJW3 by using following primer sets, #20 and #22 (ΔC60), #20 and #25 (N), #23 and #26 (central), and #24 and #27 (C), respectively. These PCR fragments were cloned into pSM671 at EcoRI/SalI site and used as bait. pSM671 was derived from pACT2 (Clontech), but its *GAL1* promoter and *GAL4AD* had been replaced by *ADH1* promoter and *LexABD* of pEG202 (Funakoshi) (Y. Nakajima and S. Mimura, unpublished plasmid) (Mimura et al., 2010), respectively. The constructs of the amino terminus of Mcm2 (amino acid: 1-192), MCM domain of Mcm2 (amino acid: 193-868), the amino terminus of Mcm6 (amino acid: 1-100), MCM domain of Mcm6 (amino acid: 101-842), and the carboxy terminus of Mcm6 (amino acid: 843-1017) were amplified from pSM379 (Mcm2) and pNYN30 (Mcm6), respectively, using following primer sets, #28 and #29 (Mcm2 N), #30 and #31 (Mcm2 MCM), #32 and #33 (Mcm6 N), #34 and #35 (Mcm6 MCM), and #36 and #37 (Mcm6 C),

respectively. Then, these PCR products were cloned into AscI/NotI sites of pNYN31 (Y. Nakajima and S. Mimura, unpublished plasmid) after removing *MCM7* ORF from pNYN31 and used as prey. pNYN31 derived from pJG4-5 (Clontech) in which *GAL1* promoter was replaced with *ADH1* promoter (Mimura et al., 2010). These bait and prey plasmids were transformed into the wild type host cell, L40 (*MATa his3-delta200 trp1-901 leu2-3112 ade2 lys2-801am LYS2::(lexAop)4-HIS3 URA3::(lexAop)8-lacZ GAL4*). The transformants were selected on SD-Leu-Trp plate. The transformants were isolated and grown in SC-Leu-Trp media and $1.5x10^5$ cells were spotted on either SC-Leu-Trp or SC-Leu-Trp-His or SC-Leu-Trp-His+3-AT (final concentration is 0.2 mM) plates, respectively. Spotted cells were grown at 30˚C for 2-4 days. The oligos and plasmids used in this assay is shown in Table 3 and 4, respectively.

Results

A novel conditional allele, *mcm10-1-aid*, shows a pronounced defect in DNA replication

To see defects caused upon Mcm10 depletion *in vivo*, I wished to use a tight conditional *mcm10* allele. I and others noticed that conventional ts alleles of *mcm10*, *mcm10-1,* and *mcm10-43,* enter the S phase gradually and duplicate most genomic DNA at later time points at the restrictive temperature (Figure 4b) (Kawasaki et al., 2000). Such a phenotype would obscure the defect

upon Mcm10 inactivation and make the interpretation of results more difficult. Moreover, these alleles confer different defects at the initiation of replication (Homesley et al., 2000; Sawyer et al., 2004). I therefore tried to construct a better conditional strain using the AID technology (Nishimura et al., 2009). With this system, a protein of interest fused with the aid tag is polyubiquitinized by SCF^{TIR1}, which is an E3 ubiquitin ligase in the presence of auxin (Figure 3). As a result, it would be degraded rapidly by the ubiquitin-proteasome pathway. However, the *mcm10-aid* cells showed a leaky phenotype (Figure 4a, *mcm10-aid*). I thus constructed the *mcm10-1-aid* cells that does not grow on agar medium containing auxin without a temperature shift (Figure 4a, *mcm10-1-aid*). Importantly, the *mcm10-1-aid* cells showed a more pronounced defect at the G1-S transition than the original *mcm10-1* cells under the restrictive conditions (Figure 4b). Under the permissive conditions, the protein level of Mcm10-1-aid was 15 % of that of Mcm10 in the wild type cells consistent with the previous report showing that the Mcm10-1 level is lower at the permissive temperature (Figure 4c) (Sawyer et al., 2004). After auxin addition, the protein level of Mcm10-1-aid was lowered to 2 % compared with the Mcm10 level in the wild type cells within 30 min. Strikingly, the protein level of Pol1 (also called Cdc17), the catalytic subunit of Polα, was not affected after Mcm10 depletion in the *mcm10-1-aid* background, unlike with the case of *mcm10-ts* cells (Figure 5) (Ricke and Bielinsky, 2004, 2006). I also found that slow migrating Pol12, the second largest subunit of Polα, had accumulated in the absence of Mcm10, suggesting that the cells arrested in the presence of

high CDK activity that phosphorylates Pol12 (Foiani et al., 1995). I thus concluded that the lethality caused upon Mcm10 depletion was not because of the destabilization of Polα but because of another defect in DNA replication in the *mcm10-1-aid* strain.

Mcm10 plays an essential role in the initiation but may not play a major role in the elongation

Previous reports using conditional *mcm10-ts* mutants have shown that Mcm10 is required for both replication initiation and elongation (Homesley et al., 2000; Ricke and Bielinsky, 2004). To see whether the same is true in the *mcm10-1-aid* cells, I conducted cell-cycle block and release experiments. I used an AID mutant of *cdc45*, *cdc45-aid*, as a control showing defects in both replication initiation and elongation (Nishimura et al., 2009; Tercero et al., 2000). The *mcm10-1-aid* and *cdc45-aid* cells were initially synchronized in G1 or early S phase, using the mating pheromone α-factor or hydroxyurea (HU), respectively, before Mcm10 depletion. The cells were then released from the cell cycle block to follow the duplication of genomic DNA by flow cytometry. When the *mcm10-1-aid* cells were released from G1 phase with Mcm10, the cells duplicated most of genomic DNA by 90 min (Figure 6a, + Mcm10). On the other hand, they arrested their cell cycle at G1/S transition even at 90 min without Mcm10 (Figure 6a, - Mcm10). Taking the fact that *cdc45-aid* behaved in a similar fashion (Figure 6b), these results suggest that *mcm10-1-aid* cells had a pronounced defect in the initiation and/or the

elongation. When the *mcm10-1-aid* cells were released from early S phase in the presence of Mcm10, they resumed DNA replication and duplicated most of DNA by 90 min (Figure 6c, + Mcm10). Interestingly, even without Mcm10 the cells carried out DNA replication with a slightly slower kinetics and a small proportion of cells completed mitosis at 150 min (Figure 6c, - Mcm10). The slight delay of DNA replication from early S block is possibly due to the inactivation of late-firing origins. On the contrary, the *cdc45-aid* cells did not reach to 2C even at 150 min when released from early S phase without Cdc45, showing that these cells have a defect in the elongation (Figured) (Tercero et al., 2000). An apparent reason why Mcm10 has been thought to be involved in the elongation is that Mcm10 was reported to be required for stabilizing Polα (Ricke and Bielinsky, 2004). However, Polα was not destabilized in *mcm10-1-aid* in my hands (Figure 5). I therefore concluded that Mcm10 plays an essential role in the initiation but may not play a major role in the elongation.

S-CDK- and Cdc45-dependent association of Mcm10 with origins

To know when Mcm10 associate with replication origins in the initiation, I used a chromatin immunoprecipitation (ChIP) assay combined with a quantitative real-time PCR and examined Mcm10 association at two early origins, *ARS305* and *ARS306*, non origin region, apart 9 kb from *ARS305,* and late origin *ARS501* (Figure 7) (Calzada et al., 2005; Kanemaki and Labib, 2006). Budding yeast cells expressing a 5xFLAG-tagged Mcm10 (Mcm10-5FLAG) were synchronized in G1 phase and then released into S phase (Figure 8a).

The samples were taken at 0, 30, 45, and 60 min to examine Mcm10 association with *ARS305*, *ARS306,* and *ARS501* (Figure 8b). The association signal of Mcm10 with *ARS305* and *ARS306* sharply increased at 30 min and quickly declined later. At the late-firing origin *ARS501,* a broader association peak was observed at 30 and 45 min, consistent with the observation that *ARS501* is activated in late S phase (Ferguson et al., 1991). Under my experimental conditions, Mcm10 association with origins in the G1 phase was not observed. These results suggest that Mcm10 associates with origins during the initiation process.

Because S-CDK activation is essential for the initiation (Tanaka et al., 2007; Zegerman and Diffley, 2007), I next investigated whether the Mcm10 association with origins requires S-CDK activity. To inactivate S-CDK, the CDK inhibitor Sic1ΔNT protein was expressed from the galactose-inducible *GAL1-10* promoter in cells synchronized in G1 phase before releasing into S phase (Drury et al., 1997). The cells were then released from G1 phase. Under this condition, the cells did not duplicate their genomic DNA (Figure 8c). The Mcm10 association with *ARS305*, *ARS306,* and *ARS501* were barely detected in the absence of S-CDK activity, suggesting that S-CDK activity is required for the Mcm10 loading to origins *in vivo* (Figure 8d). Cdc45 stably binds Mcm2-7 following S-CDK activation *in vivo* (Zou and Stillman, 1998), and is required for Mcm10 loading *in vitro* (Heller et al., 2011). I therefore wondered whether Cdc45 is required for Mcm10 association with origins *in vivo*. To test this, I used the *cdc45-aid* cells for Cdc45 depletion (Figure 4a)

(Nishimura et al., 2009). After synchronization in the G1 phase, degradation of Cdc45-aid was induced by auxin addition before releasing the cells from the G1 block. In the absence of Cdc45, the cells did not duplicate DNA (Figure 9b, - Cdc45) (Tercero et al., 2000). As with the case of S-CDK inactivation, the association of Mcm10 with *ARS305* and *ARS306* was lost in the absence of Cdc45 (Figure 9b, - Cdc45), showing that Cdc45 is required for the Mcm10 association with origins.

In the control experiments described above (Figures 8b and 9b), no significant Mcm10 association with the non-origin loci was detected using quantitative PCR. These results suggest that Mcm10 may associate with the replisome transiently. To test whether Mcm10 moves stably with the replisome, I investigated the association of Cdc45 and Mcm10 with *ARS305* and non-origns by ChIP in cells expressing an 18xMyc-tagged Cdc45 (Cdc45-18Myc) and Mcm10-5FLAG, simultaneously. After synchronization in the G1 phase, the cells were released into HU-containing medium to slow fork progression (Figure 10a). In accordance with previous reports (Aparicio et al., 1997; Kamimura et al., 2001a; Kanemaki and Labib, 2006), Cdc45 associated with *ARS305* in the G1 phase, and the association signal increased at 30 min upon activation of the origin in S phase (Figure 10b). Then, Cdc45 association signal moved to the + 2kb locus at 45 to 60 min and shifted to the + 4kb locus at 60 to 75 min, showing that Cdc45 moved away from *ARS305* following the formation of the replisome (Aparicio et al., 1997). However, at the + 6kb locus, no significant Cdc45 signal was detected, indicating that

replication forks did not reach by this locus under this experimental condition. Mcm10 association was detected at *ARS305* at 30 min similar to Cdc45 (Figure 10c). However, no obvious signal was observed at + 2kb and + 4kb locus compared to + 6kb, except for the signal at + 2kb at 60 min. Taking into account that Cdc45 is a component of CMG (Ilves et al., 2010; Moyer et al., 2006), these results support the hypothesis that Mcm10 might not be integral component of replisome. My interpretation is also consistent with the observation that the cells depleted of Mcm10 in early S phase carried out DNA replication (Figure 6c). All of these results are consistent with our conclusion that Mcm10 plays an essential role in the initiation, but may not in the elongation.

A stable CMG complex forms and stays at origins in the absence of Mcm10

S-CDK- and Cdc45-dependent association of Mcm10 with origins as shown in Figures 8d and 9b suggests two possibilities; CMG formation and Mcm10 association occur in a mutually dependent manner or Mcm10 is required after CMG formation. To distinguish between these two possibilities, I tested Cdc45 association with origins in the presence or absence of Mcm10. Cells expressing a 5xFLAG-tagged Cdc45 (Cdc45-5FLAG) in the *mcm10-1-aid* background were initially arrested in the G1 phase. Mcm10 was degraded before releasing from the G1 block, and the samples were collected at 0, 30, 45, and 60 min. Under this condition, the cells induced for Mcm10 depletion

did not duplicate DNA (Figure 11a). Cdc45 association with *ARS305/ ARS306,* and the non-origin region, apart 9kb from *ARS305* were quantified by ChIP (Figure 11b). In the presence of Mcm10, Cdc45 association was detected at the origins in the G1 phase as it was shown in Figure 10b (Figure 11b, +Mcm10). The Cdc45 association signal at *ARS305* and *ARS306* then increased at 30 min followed by a sharp decline at 45 min. At 30 min, Cdc45 association was concomitantly detected at the + 9kb loci, suggesting that the replisome containing Cdc45 was travelling (Aparicio et al., 1997). In the absence of Mcm10, Cdc45 association was detected at *ARS305* and *ARS306* in G1 phase as in the control, showing that Mcm10 is not functionally required for the initial association of Cdc45 (Figure 11b, - Mcm10). However, the Cdc45 signal reached to a very high level at 30 min and was maintained even at 60 min, suggesting that S-CDK executed the initiation reaction, but Cdc45 remained at *ARS305* and *ARS306*. Decline of the Cdc45 signal from 30 to 60 min might be because of an abortive loss of Cdc45 from the origin, leakage caused by residual Mcm10, or both. These results support the hypothesis that Mcm10 plays a role independent of CMG formation.

If Mcm10 plays a role independent of CMG formation, a CMG complex should form without Mcm10. I therefore analyzed CMG formation by immunoprecipitating the GINS Psf2 subunit in the presence or absence of Mcm10. Cells expressing both a 5xFLAG-tagged Psf2 (Psf2-5FLAG) and a 6xHA-tagged Mcm4 (Mcm4-6HA) in the *mcm10-1-aid* background were synchronized in G1 phase. In the presence or absence of Mcm10, the cells

were released into HU containing medium (Figure12a). Mcm10 depletion was verified by a non-increase of DNA content in the cells released into medium without HU (Figure 12b, - HU, compare + and - Mcm10). In both conditions, slow-migrating Mcm4 was detected only in S phase extracts, suggesting that Mcm4 was phosphorylated by DDK (Figure 12c, lanes 3 and 4) (Francis et al., 2009; Sheu and Stillman, 2006). Psf2 was then immunoprecipitated from the extracts prepared from the cells arrested in G1 or early S phase. Intriguingly, only the S phase-specific slow-migrating Mcm4 protein was co-immunoprecipitated with Psf2 both in the presence and absence of Mcm10, strongly suggesting that a CMG complex formed even without Mcm10 (Figure 6e, lanes 7 and 8). I also noticed that Mcm4 was co-precipitated 16% less efficiently in the absence of Mcm10, implying that Mcm10 might have a minor role for CMG formation (Figure 12c, compare lanes 7 and 8). The immunoprecipitants were unaffected after a 500 mM KOAc or NaCl wash showing that a CMG complex formed without Mcm10 is salt resistant (Figure 12d and e). Taking the observation that Cdc45 remained at origins (Figure 11b), I concluded that a stable CMG formed and stayed at origins in the absence of Mcm10.

Origin unwinding is defective in the absence of Mcm10

My results shown above prompted me to test whether downstream events following CMG formation would be affected in the absence of Mcm10. Because CMG is the replicative helicase (Ilves et al., 2010; Moyer et al., 2006),

origin unwinding is expected after CMG formation. I therefore analyzed the association of the single-strand binding RPA protein as an indicator of DNA unwinding. Cells expressing a 5xFLAG-tagged Rfa1 (Rfa1-5FLAG), the largest subunit of RPA, in the *mcm10-1-aid* background were synchronized in the G1 phase, followed by release from the G1 block in the presence or absence of Mcm10. Note that I did not use the replication inhibitor HU, which induces RPA accumulation at unwound origins (Katou et al., 2003; Tanaka and Nasmyth, 1998). The DNA content of the cells stayed at 1C up to 60 min in the absence of Mcm10, showing that Mcm10 was depleted efficiently to block DNA replication in the cells (Figure 13a). In the presence of Mcm10, Rfa1 association was detected at both *ARS305* and *ARS306* mainly at 30 min, suggesting that origin unwinding occurred at this time (Figure 13b, + Mcm10). Rfa1 association was also detected at the non-origin at 30 and 45 min, suggesting that forks are travelling at the locus. Strikingly, the loading of Rfa1 on *ARS305* and *ARS306* was severely reduced in the absence of Mcm10 (Figure 13b, - Mcm10), suggesting that origin unwinding sufficient to load RPA was defective in the cells. Consistent with the observation that Cdc45 stays at origins without Mcm10 (Figure 11b), Rfa1 was not detected above the background level at the non-origins throughout the time course. Even though there was a clear defect, a slow and low Rfa1 accumulation was observed at the origins. I interpret this as being caused by incomplete Mcm10 depletion.

If an efficient origin unwinding was defective in the absence of Mcm10, the intra-S checkpoint activation requiring ssDNA exposure should also be

defective without Mcm10 (Zou and Elledge, 2003). To test this, Rad53 phosphorylation was investigated in cells depleted of Mcm10 or Cdc45. I initially synchronized the *mcm10-1-aid* or *cdc45-aid* strain in the G1 phase. After Mcm10 or Cdc45 depletion, the cells were released into HU containing medium to activate the intra-S checkpoint. I took the samples at 0, 45, 60, and 75 min and analyzed Rad53 phosphorylation (Figure 14a). In the presence of Mcm10 and Cdc45, a slow-migrating form of Rad53 was accumulated at the later time points (Figure 14b and c, left), suggesting that ssDNA was exposed after establishment of the replisome. In sharp contrast, the mobility shift of Rad53 was severely diminished in the absence of Mcm10 or Cdc45 (Figure 14b and c, right). Taking into account that Cdc45 is a CMG component and is thus essential for origin unwinding (Ilves et al., 2010; Moyer et al., 2006), the results in Figure 14c reinforce the hypothesis that origin unwinding is defective in the cells without Mcm10. Taken together with the results showing a stable CMG stayed at origins and the downstream events are severely diminished in the absence of Mcm10 (Figures 11-14), I concluded that Mcm10 plays an essential role in a time window after CMG formation and before origin unwinding (Figure 20a).

Polα loading in the absence of Mcm10

After origin unwinding, Polα is reported to bind unwound origins (Tanaka and Nasmyth, 1998). Therefore I expected that Polα does not associate with early firing origins without Mcm10. To confirm this, cells expressing a

5xFLAG-tagged Pol1 (Pol1-5FLAG) in the *mcm10-1-aid* background were synchronized in the G1 phase before releasing into S phase with or without Mcm10 (Figure 15a). In the presence of Mcm10, the Polα catalytic subunit Pol1 was detected at *ARS305* and *ARS306* from 30 min until Pol1 association declined to the near background level at 60 min (Figure 15b, + Mcm10). Pol1 was also detected at the + 9kb locus at 30 and 45 min suggesting that Polα was traveling as a part of the replisome (Calzada et al., 2005; Katou et al., 2003; Tanaka and Nasmyth, 1998). Intriguingly, when Mcm10 was depleted I found that Pol1 was detected at both *ARS305* and *ARS306* at 30 min and stayed at high even at 60 min (Figure 15b, - Mcm10). Consistently, Pol1 was not detected at the + 9kb locus throughout the time course under this condition. Unexpectedly, these results suggest that Polα associates with origins even before origin unwinding.

The results of Pol1 ChIP shown above suggest that Polα may physically interact with CMG formed in the absence of Mcm10. To study physical interaction between Polα and CMG, I immunoprecipitated Psf2, a component of GINS, either in the presence or absence of Mcm10. The cells expressing Psf2-5FLAG was synchronized in the G1 phase before releasing into HU containing medium, following the protocol shown in Figure 12a. Psf2 was immunoprecipitated from extracts prepared from either G1 or S phase arrested cells. Previous report showed that Pol1 was co-immunoprecipitated with CMG only under a low salt condition (Gambus et al., 2009). Under a similar experimental condition, Pol1 was co-precipitated with Psf2 in S phase

in the presence of Mcm10, showing that Polα associates with CMG at forks (Figure 16, lane 7). However, in the absence of Mcm10, Pol1 was not significantly co-precipitated with Psf2 in S phase, indicating that Polα does not stably associate with GMG before origin unwinding (Figure 16, lane 8). Note that I did not use the cross-linker formaldehyde that was used in the Pol1 ChIP assay (Figure 15b). Taking the fact that Pol1 was captured at origins in the ChIP assay, these results may suggest that Polα loading onto replication origins occurs in two steps. Initially, Polα may weakly associate with CMG before origin unwinding. This weak association can be captured only by the use of crosslinker. Subsequently, after Mcm10 plays an essential role for origin unwinding, Polα stably associates with CMG at replication fork. Although I favor the interpretation shown above, it is still possible that incomplete Mcm10 depletion in the *mcm10-1-aid* strain might have caused Polα accumulation at *ARS305* and *ARS306* in the ChIP assay (Figure 15b, - Mcm10). In fact, a low level of Rfa1 slowly accumulated at this origin in the absence of Mcm10, suggesting that Mcm10 depletion was not complete in *mcm10-1-aid* (Figure 15b, - Mcm10).

Mcm10 strongly interacts with Mcm2 and Mcm6

To characterize the role of Mcm10 in a time window after CMG formation and before origin unwinding, it is useful to investigate how Mcm10 interacts with other replication factors. It has been reported that Mcm10 physically interacts with CMG components, Mcm2-7, Cdc45, and GINS (Gambus et al., 2006;

Merchant et al., 1997; Sawyer et al., 2004). To only detect the essential interactions of Mcm10, I tried to identify minimum region of Mcm10 required for the cell viability. The conserved central region of Mcm10 has the OB-fold/Zn-finger domain and it has been reported that the mutations in the Zn-finger domain causes temperature sensitive or cell death (Cook et al., 2003; Homesley et al., 2000; Warren et al., 2008). Thus, it has been proposed that the conserved central region is essential for the cell viability. In addition, there are two NLSs in the C-terminal region of Mcm10 and, at least, one of two is sufficient to support the cell viability (Figure 17a) (Burich and Lei, 2003). Taken together with all these information, I constructed two types of C- and one N-terminus truncated mutants of Mcm10 (Figure 17a). To avoid loss of function by losing one NLS, I fused GFP and the SV40 NLS to these each mutant. These proteins were expressed from a low copy plasmid, pRS414, under the control of an *MCM10* promoter in the cells, the endogenous *MCM10* gene was deleted but wild type Mcm10 was expressed from a *URA3* containing plasmid. I confirmed that these mutant proteins were expressed equally in the cells (Figure 17b). In order to study whether these Mcm10 mutants would complement the wild type Mcm10 protein, I grew the cells on plates containing 5-fluoroorotic acid (5-FOA), on which only the cells that had lost the *URA3* plasmid containing the wild type *MCM10* gene can proliferate. As a result, truncation mutant lacking the C-terminal 60 amino acids (ΔC60) and N-terminal 150 amino acids (ΔN150), respectively, complemented the loss of *MCM10* (Figure 17c, -Trp+5-FOA), whereas the mutant lacking the

C-terminal 107 amino acids (ΔC107) did not. These results suggest that C-terminus region of Mcm10 is required for its essential role. Thus, I used ΔC60 mutant to investigate the interactions for the essential role of Mcm10.

In this study, I found that Mcm2-7, Cdc45, GINS, Polε, Ctf4 and Polα associate with origins in a time window of Mcm10 function (Figure 20a, **ii**). Furthermore, it has been reported that homo complex formation of Mcm10 is important for its essential function in budding yeast (Cook et al., 2003). Thus, I performed yeast two-hybrid (Y2H) assay to see the interactions of ΔC60 mutant with Mcm2-7, Cdc45, GINS, Ctf4, Polα, and Mcm10. As a result, I found that the ΔC60 mutant interacts with Mcm2, Mcm6, Mcm7, and Pol1 (Figure 17d, -His). Especially, among these interactions, the interactions of ΔC60 with Mcm2 and Mcm6 were still observed even in the presence of a inhibitor of histidine synthesis, 3-asmino-1,2,4-triazole (3-AT), suggesting that the interaction of Mcm10 with Mcm2 and Mcm6 is stronger than that with Mcm7 or Pol1 (Figure 17d, -His+3-AT).

The central domain of Mcm10 containing the OB-fold/Zn-finger motif is sufficient to interact with non-MCM domains of Mcm2 and Mcm6

To investigate more detail about the interactions of Mcm10 with Mcm2 and Mcm6, I divided Mcm10 into three regions, N-terminal (a.a. 1-150), central (a.a. 151-370) and C-terminal (a.a. 371-571), respectively, based on the secondary structure prediction (psipred) and secondary structure-based profile-profile alignment (HHpred) (Figure 18a). I carried out Y2H assay by using these

three divided regions of Mcm10 as a bait. As a result, no interaction was observed between the N-terminal region and Mcm2/6 (Figure 18b, -His), suggesting that N-terminal region of Mcm10 is not involved in the interaction between Mcm10 and Mcm2/6. It is consistent with the result that the ΔN150 mutant complements *Δmcm10* (Figure 17c). On the other hand, the central region interacted with both Mcm2 and Mcm6 (Figure 18b, -His). Unfortunately, the cells expressing the C-terminal region of Mcm10 showed a growth defect especially in the cell co-expressing Mcm6 (Figure 18b, +His). Even under this condition, the interaction of the C-terminal region with Mcm2 was observed, suggesting that Mcm2 interacts with both central and C-terminal region. In summary, the central region of Mcm10 is sufficient to interact with Mcm2 and Mcm6 (Figure 18b, -His).

Conversely, I next investigated that interaction regions of Mcm2 or Mcm6 associates with the central region of Mcm10. The Mcm family proteins including Mcm2 and Mcm6 possess the MCM domain in which the walker A and B, and R-finger motifs for ATP hydrolysis are conserved. In addition, Mcm2, Mcm4 and Mcm6 have an unstructured extension at the N-terminus, which is phosphorylated by DDK during S phase (Bruck and Kaplan, 2009; Devault et al., 2008; Sheu and Stillman, 2006, 2010). Based on these previous reports, secondary structural analysis and its based profile-profile alignment by using the psipred and HHpred softwere, respectively. I made truncations of Mcm2 and Mcm6 (Figure 19a). To study whether these truncations interacts with Mcm10 central region, I carried out Y2H assay. As

a result, I found that N-terminal fragment of Mcm2 (a.a. 1-192) and the C-terminal fragment of Mcm6 (a.a. 843-1017) interact with central region of Mcm10 (Figure 19b, -His). Furthermore, in the presence of 3-AT, only the N-terminal fragment of Mcm2 showed a interaction with the central region of Mcm10 (Figure 19b, -His+3-AT).

In summary, I found that Mcm10 strongly interacts with Mcm2 and Mcm6. This interaction is mediated by the central and non-MCM domains of Mcm10 and Mcm2/6, respectively. Taken together with that Mcm10 plays a role in a time window after CMG formation before origin unwinding, it is likely that Mcm10 is involved in conformational change of Mcm2-7 during CMG activation by interacting with Mcm2 and Mcm6. I propose possible roles of Mcm10 in Discussion.

Discussion

Difference between *mcm10-1-aid* and previous *mcm10-ts* mutants

In order to make a tight conditional *mcm10* allele, I have combined the AID technology with the *mcm10-1* mutation (Merchant et al., 1997; Nishimura et al., 2009). I found that *mcm10-1-aid* showed tighter growth defect than *mcm10-aid* in the presence of auxin (Figure 4a). A previous paper showed a similar synthetic enhancement by combining the temperature-sensitive degron method with the *sld3-7* mutation (Kanemaki and Labib, 2006). In case when these inducible degron methods do not produce tighter mutants, combination

with a conventional mutant allele might help.

In the *mcm10-1-aid* strain, I found that Polα was not destabilized unlike with the case in the previous reports using *mcm10-ts* mutants (Figure 5 d) (Haworth et al., 2010; Ricke and Bielinsky, 2004, 2006). This apparent contradiction could be due to the nature of mutants and/or the experimental condition. In the previous analysis, Mcm10 was inactivated at the higher restrictive temperatures in *mcm10-ts* cells. As it has been shown that the Polα catalytic Pol1 subunit is not stable *in vitro* (Lucchini et al., 1985) and Mcm10 interacts with Polα (Figure 17d) (Fien et al., 2004; Ricke and Bielinsky, 2006; Warren et al., 2009), Pol1 might be more affected after drastic shift to higher temperatures especially when Mcm10 was inactivated. On the other hand in this study, Mcm10 depletion was induced by auxin addition at the constant temperature of 24^{o}C. It is also noteworthy that Mcm10 was depleted within 30 min in *mcm10-1-aid*, in contrast to relatively slow Mcm10 depletion in the *mcm10-1* and *mcm10-43* strains at 36^{o}C (Sawyer et al., 2004). A previous report showed that fast depletion of target proteins was important to see the initial defect avoiding secondary effects (Kanemaki et al., 2003).

Mcm10 may not be an integral replisome component

In this study, I revealed that the *mcm10-1-aid* cells had a profound defect in the initiation but didn't have a strong defect in the elongation (Figure 6a and c). In support of these results, I found that Mcm10 was detected at origins but not stably away from origins by ChIP (Figures 8b, 9b, and 10c). I therefore favor

the idea that Mcm10 is not a stable replisome component thus do not play a major role for normal replication elongation. Previous reports do not deny this hypothesis. First, Mcm10 was detected at a low level in the stalled replisome complex in *Xenopus* but not a part of the replicative helicase complex when decoupled from DNA polymerases (Pacek et al., 2006). Second, Mcm10 was detected at origins in human cells but it was not conclusive whether Mcm10 moved away from origins as a replisome component (Karnani and Dutta, 2011). Third, GINS purified from budding yeast at a high salt condition contained Mcm10 but other replisome components were not co-purified under the same condition (Gambus et al., 2006). These reports suggest a possibility that Mcm10 is not an integral component of the replisome. It is still possible that Mcm10 weakly associates with the replisome or is recruited to forks when required. In budding yeast, Mcm10 is required for the forks passage through replication origins, potential pausing sites (Merchant et al., 1997). This could be due to a fork block caused by inactive CMG staying at origins in the absence of Mcm10 (Figures 11 and 12).

Mcm10 is detected at origins after a stable CMG formation

Previous reports agree that Mcm10 binds to origins in S phase (Gregan et al., 2003; Heller et al., 2011; Izumi et al., 2000; Ricke and Bielinsky, 2004; Wohlschlegel et al., 2002). However, there is not a consistent view of whether Mcm10 binds to origins in G1 phase when S-CDK is inactive. In this study, I revealed that Mcm10 associates with origins in an S-CDK and Cdc45

dependent manner and a stable CMG is formed without Mcm10 (Figures 9b, 11b, 12c-e). My *in vivo* results fits to the recent *in vitro* observation that Mcm10 binds to origins after the loading of Cdc45 and GINS (Heller et al., 2011). A recent fission yeast study also found that Mcm10 bound to origins after Rad4/Cut5 (the Dpb11 homolog) loading (Taylor et al., 2011). I therefore favor the view that Mcm10 loads to origins after a stable CMG formation *in vivo*. However, I do not completely rule out the possibility that Mcm10 is recruited to origins from G1 phase as it is formally possible that my ChIP condition might not crosslink the interaction between Mcm10 and origins for a spatial hindrance in pre-RC.

Mcm10 plays an essential role in a novel step of the initiation

In contrast to the previous reports showing that Mcm10 is required for Cdc45 loading to origins (Gregan et al., 2003; Sawyer et al., 2004; Wohlschlegel et al., 2002), I revealed that Mcm10 is required after the formation of a stable CMG complex as with case of the recent *in vitro* study (Heller et al., 2011). Three lines of evidence support my conclusion that Mcm10 is dispensable for the stable engagement of CMG. Firstly, Cdc45 was recruited to origins but stayed at later time points in the absence of Mcm10 (Figure 11b). Increase of Cdc45 ChIP signal in S phase suggests that pre-RC conversion was initiated but stacked in the middle of the process. Secondly, my Psf2 IP from S phase extracts identified only phospho-Mcm4 even in the absence of Mcm10 (Figure 12c and d). It has been reported that Mcm4 N-terminal phosphorylation is

required for the stable association of Cdc45 and GINS to Mcm2-7 by suppressing an inhibitory activity in Mcm4 (Sheu and Stillman, 2006, 2010). Thirdly, a CMG complex made without Mcm10 was salt resistant even at 500 mM KOAc or NaCl (Figure 12d and e).

Even though a stable CMG complex was made in the cells without Mcm10, RPA loading and the intra-S checkpoint were defective (Figures 13b and 14b). This strongly suggests that CMG formed after S-CDK activation has to be activated in the presence of Mcm10 in order to expose ssDNA enough to load RPA. I therefore propose that there is a novel step after the stable engagement of CMG at origins, in which Mcm10 plays an essential role before the establishment of the active replisome (Figure 20a).

Polα may associate with replication origins in a two-step mode

Pol1, the catalytic subunit of Polα, accumulated at origins in the absence of Mcm10, even though cells showed a defect in origin unwinding (Figure 15b). I would like to propose the possibility that Polα loading occurs in two steps; Initially, Polα associates with origins weakly before origin unwinding. Subsequently, after origin unwinding, Polα association with origins becomes strong. It has been reported that Polα was found in a large complex containing CMG at forks and Ctf4 is the key factor to connect between Polα and GINS (Gambus et al., 2009). Moreover, Ctf4 associates with GINS throughout the cell cycle (Gambus et al., 2009). Thus, it is likely that Ctf4 is recruited to origins at the same time when CMG is formed. In fact, I detected

Ctf4 in the CMG complex formed without Mcm10 (Figure 12d). Thus, Polα might be initially recruited through the interaction with Ctf4 before origin unwinding. However, this interaction might be weak compared to that occurs after origin unwinding, because the interaction between Pol1 and Psf2 in S phase extract without Mcm10 was not captured by immunoprecipitation without crosslink (Figure 16). Previous report showed that Pri1, the primase subunit of Polα, binds to origins after origin unwinding (Tanaka and Nasmyth, 1998). Because they used conventional PCR to detect Pri1 ChIP assay, weak Polα association with origins might not be detectable. However, I do not rule out the possibility that slowly accumulated RPA caused by an incomplete depletion of the Mcm10-1-aid protein led Polα accumulation at origins (Figure 13b).

Possible roles of Mcm10 in the initiation reaction

It has been reported that the hexameric Mcm2-7 ring complex encircles dsDNA in pre-RC (Evrin et al., 2009; Remus et al., 2009). On the other hand, a recent report showed that Mcm2-7 in the replisome encircles ssDNA on the leading strand when it works as the replicative helicase (Fu et al., 2011). Thus, it has been proposed that there is a topological conversion of Mcm2-7 during its activation. Taken together with that Mcm10 plays a role in a time window after CMG assembly and before origin unwinding, it is likely that Mcm10 is involved in the conformational change of Mcm2-7. It has been shown that there are at least two CMG conformations; one is notched- and the

other is locked- form (Figure 20b) (Costa et al., 2011). Mcm2-7 has a gap between Mcm2 and Mcm5, and this gap in the notched form is proposed to pass ssDNA from Mcm2-7 ring (Figure 20b, **ii**). In contrast, in the locked form, the gap between Mcm2 and Mcm5 is closed, Cdc45 and GINS seal the gate and creating a hole that can accommodate ssDNA between Mcm2/5 and Cdc45-GINS sub complex (Figure 20b, **iii**). Cdt1, the Mcm2-7 loader, forms a complex with Mcm2-7 both in budding yeast and mammalian cells and plays a role in the assembly of the pre-RC (Randell et al., 2006; Tanaka and Diffley, 2002; You and Masai, 2008). Recent report showed that Cdt1 is not required for initial recruitment of Mcm2-7 but for proper stable association of double hexamer of Mcm2-7 with origin DNA (Frigola et al., 2013). Interestingly, this group also reported a possibility that Cdt1 binds to Mcm2/6 and opens Mcm2-7 ring to load Mcm2-7 onto dsDNA (unpublished observation). Taken together, it is likely that Cdt1 plays a role for topological conversion of Mcm2-7 between Mcm2-7 and DNA. In this study, I found that Mcm10 strongly interacts with Mcm2/6 (Figure 17d, -His+3-AT). Mcm2 and Mcm6 sit side-by-side, next to the gap in the Mcm2-7 complex (Figure 20b). Furthermore, in budding yeast and human, it has been reported that Cdt1 interacts with C-terminus of Mcm6, which contains the winged-helix domain (Liu et al., 2012; Wei et al., 2010; Wu et al., 2012). I found that Mcm10 also binds to the same region of Mcm6 (Figure 19b, -HIS). A recent study in budding yeast also showed the same observation (van Deursen et al., 2012). In addition, Mcm10 has the OB-fold/Zn-finger domain in its central conserved region (Warren et al., 2008),

and it has been reported that Mcm10 binds to both ssDNA and dsDNA (Eisenberg et al., 2009; Fien et al., 2004; Robertson et al., 2008). Taken together with all these information, I would like to propose as a one possibility that Mcm10 might open the Mcm2-7 ring by direct interacting with Mcm2/6 to extrude ssDNA from Mcm2-7 ring and promote Mcm2-7 transition from dsDNA to ssDNA (Figure 20b).

Another possibility is that Mcm10 might help to dissociate Mcm2-7 double hexamer. It has been reported that Mcm2-7 connects via its N-terminus by head-to-head when it forms a double hexamer in pre-RC (Figure 20a, **i**) (Evrin et al., 2009; Remus et al., 2009). On the other hand, it has been shown that single Mcm2-7 works in the replisome (Gambus et al., 2006; Yardimci et al., 2010). Thus, it has been suggested hexamer dissociates during its activation. It has been proposed that the phosphorylation of N-terminus of Mcm2-7 by DDK plays a role in this process. In this study, I found that Mcm10 strongly interacts with N-terminus of Mcm2 (Figure 19b, -His+3-AT), which contains the phosphorylation site by DDK (Bruck and Kaplan, 2009). Therefore, it is possible to think that Mcm10 might facilitate dissociation of Mcm2-7 double hexamer following phosphorylation by DDK.

Given the fact that mechanistic understanding of DNA replication in *E.coli* was greatly advanced by *in vitro* reconstitution experiment using purified replication proteins and DNA, it is possible to think that more detail function of Mcm10 will be revealed by establishing same system in eukaryotes. What I found in this study that Mcm10 functions in a time window after CMG assembly

and before origin unwinding, strongly interacts with Mcm2/6 in this process, and this interaction is mediated by the central and non-MCM domains of Mcm10 and Mcm2/6, respectively, might contribute to study the molecular role of Mcm10 by *in vitro* reconstitution system using purified mutant proteins, for example, affecting the interaction between Mcm10 and Mcm2/6 in the future. Future analysis is awaited.

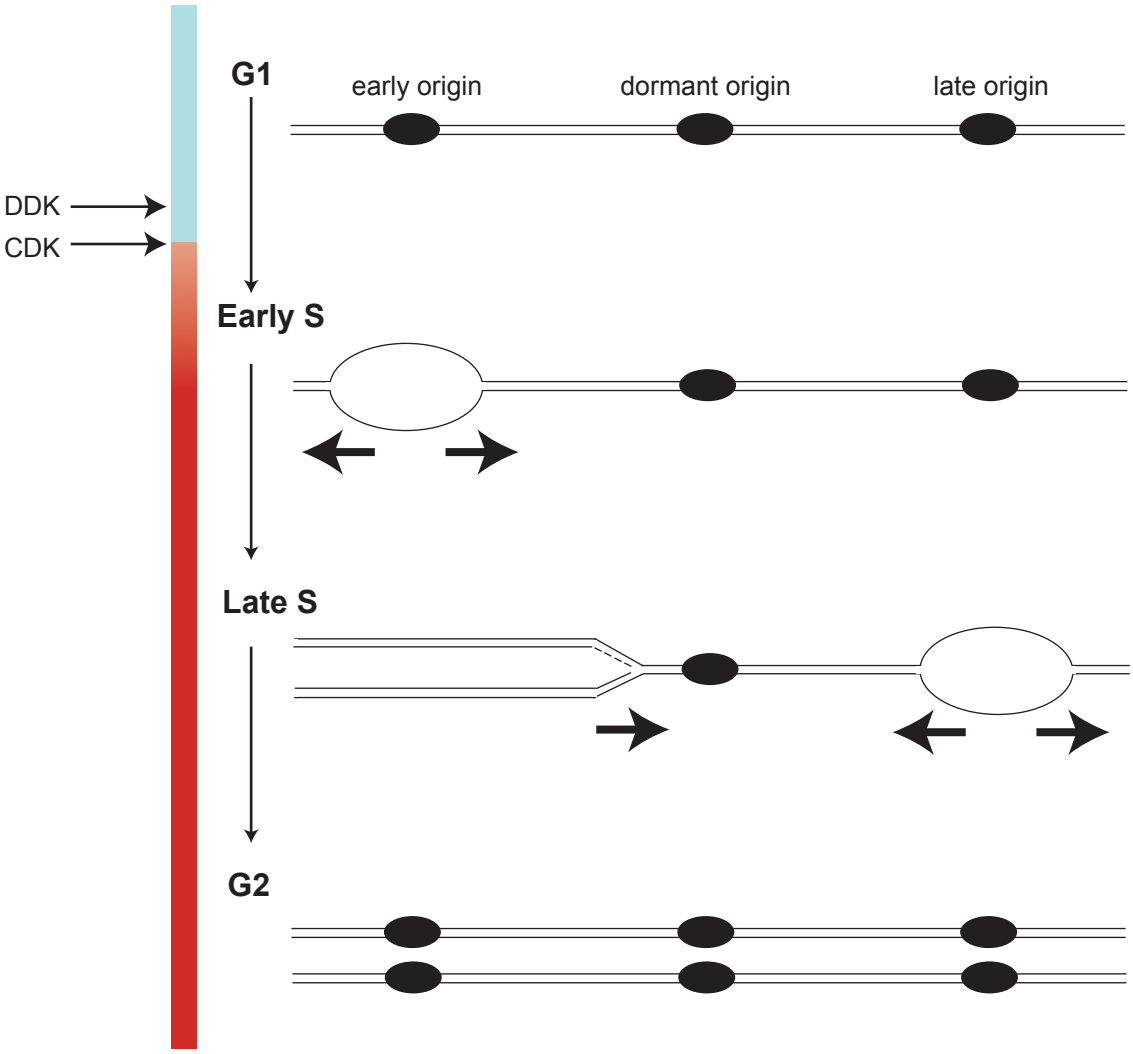
G1
early origin
dormant origin
late origin
DDK
CDK
Early S
Late S
G2

Figure 1

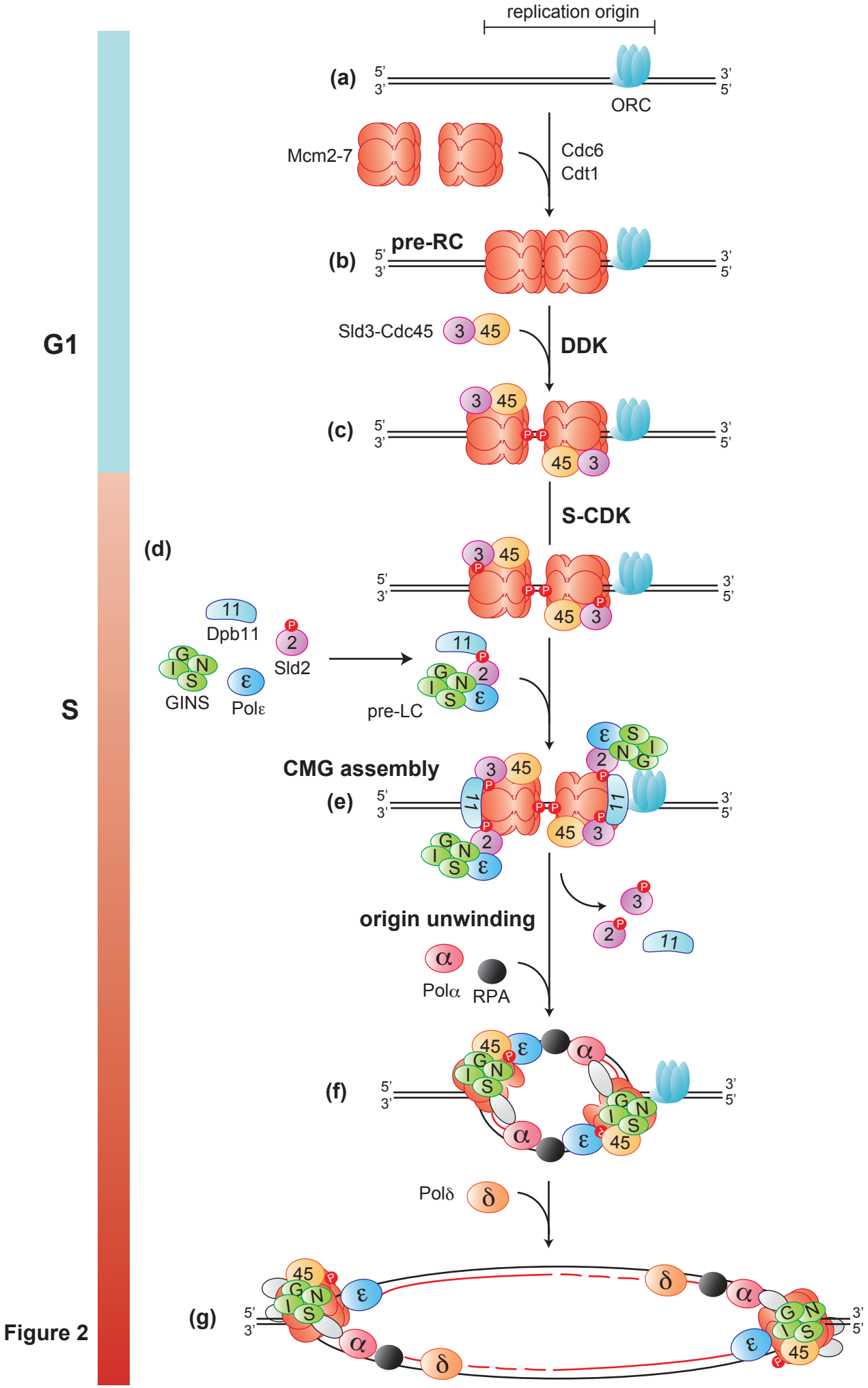
G1
S
replication origin
(a)
5'
3'
3'
5'
ORC
Mcm2-7
Cdc6
Cdt1
(b)
pre-RC
Sld3-Cdc45
3
45
DDK
(c)
S-CDK
(d)
11
Dpb11
2
Sld2
G
I
N
S
GINS
ε
Polε
pre-LC
CMG assembly
(e)
origin unwinding
α
Polα
RPA
(f)
Polδ
δ
(g)

Figure 2

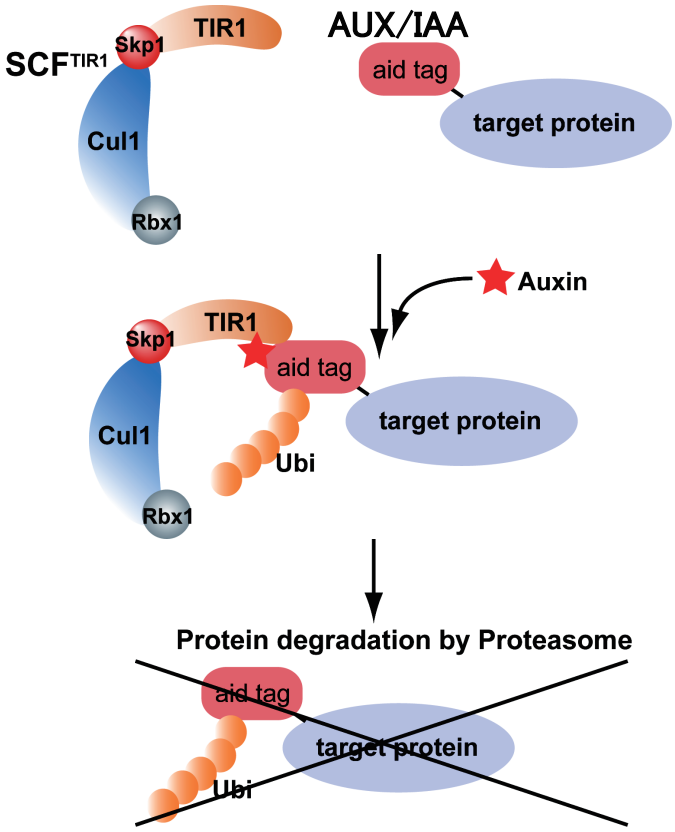
SCF TIR1
Skp1
TIR1
Cul1
Rbx1
AUX/IAA
aid tag
target protein
Auxin
Skp1
TIR1
aid tag
target protein
Cul1
Ubi
Rbx1
Protein degradation by Proteasome
aid tag
target protein
Ubi

Figure 3

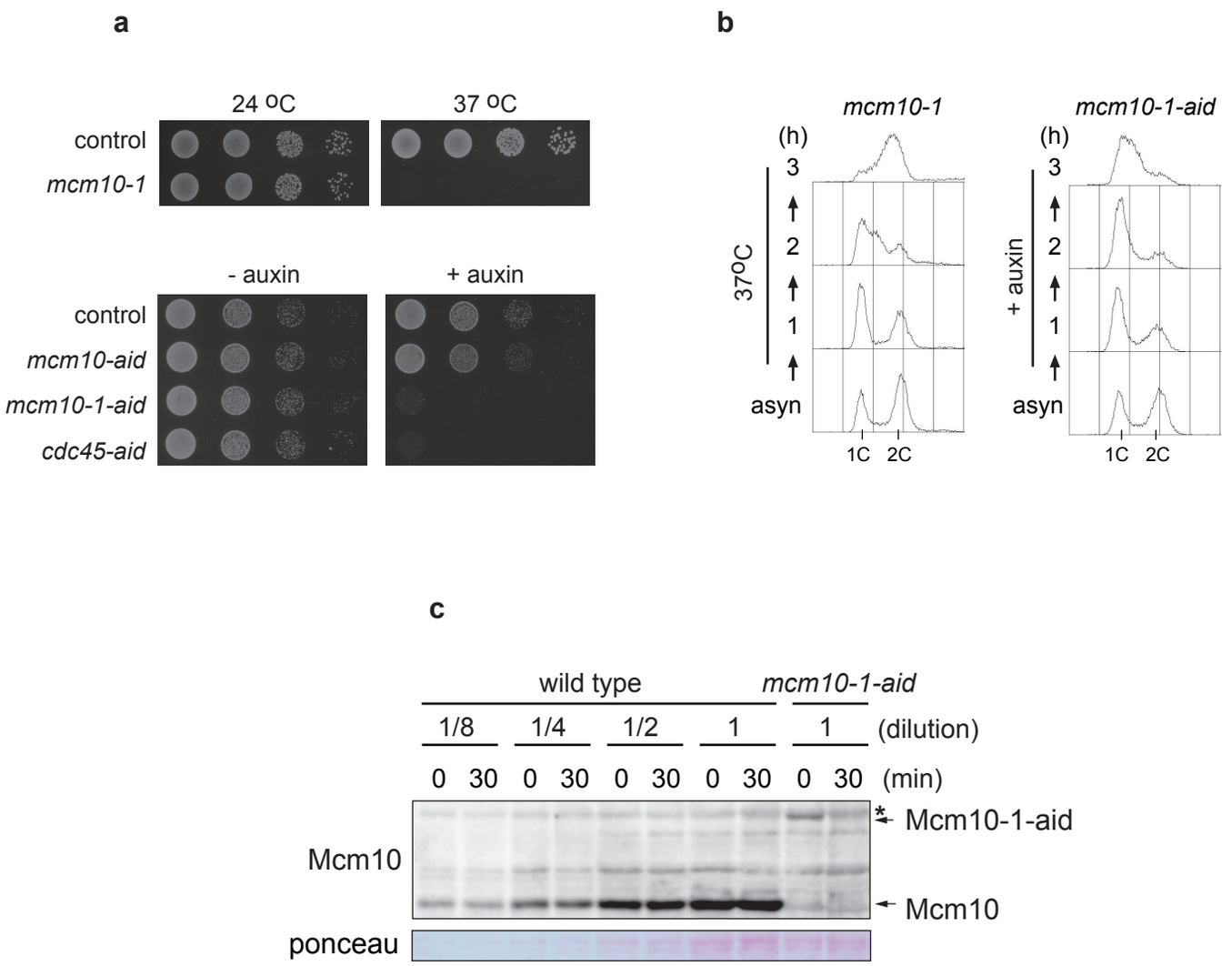
a
24 ºC
37 ºC
control
mcm10-1
- auxin
+ auxin
control
mcm10-aid
mcm10-1-aid
cdc45-aid
b
mcm10-1
mcm10-1-aid
(h)
3
2
1
asyn
37ºC
+ auxin
1C
2C
c
wild type
mcm10-1-aid
1/8
1/4
1/2
1
1
(dilution)
0 30 0 30 0 30 0 30 0 30 (min)
Mcm10
Mcm10-1-aid
Mcm10
ponceau

Figure 4

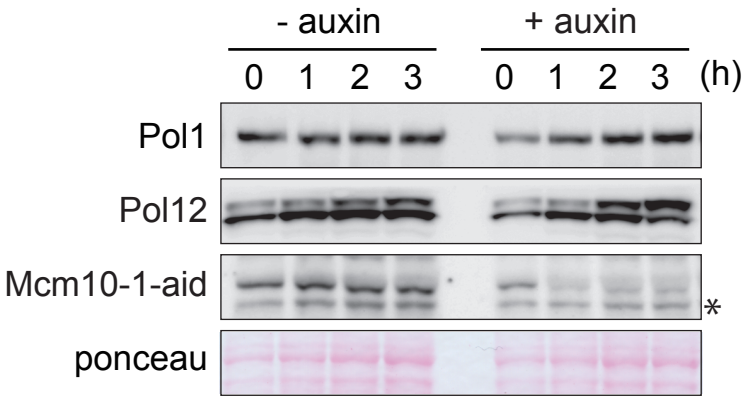

Figure 5

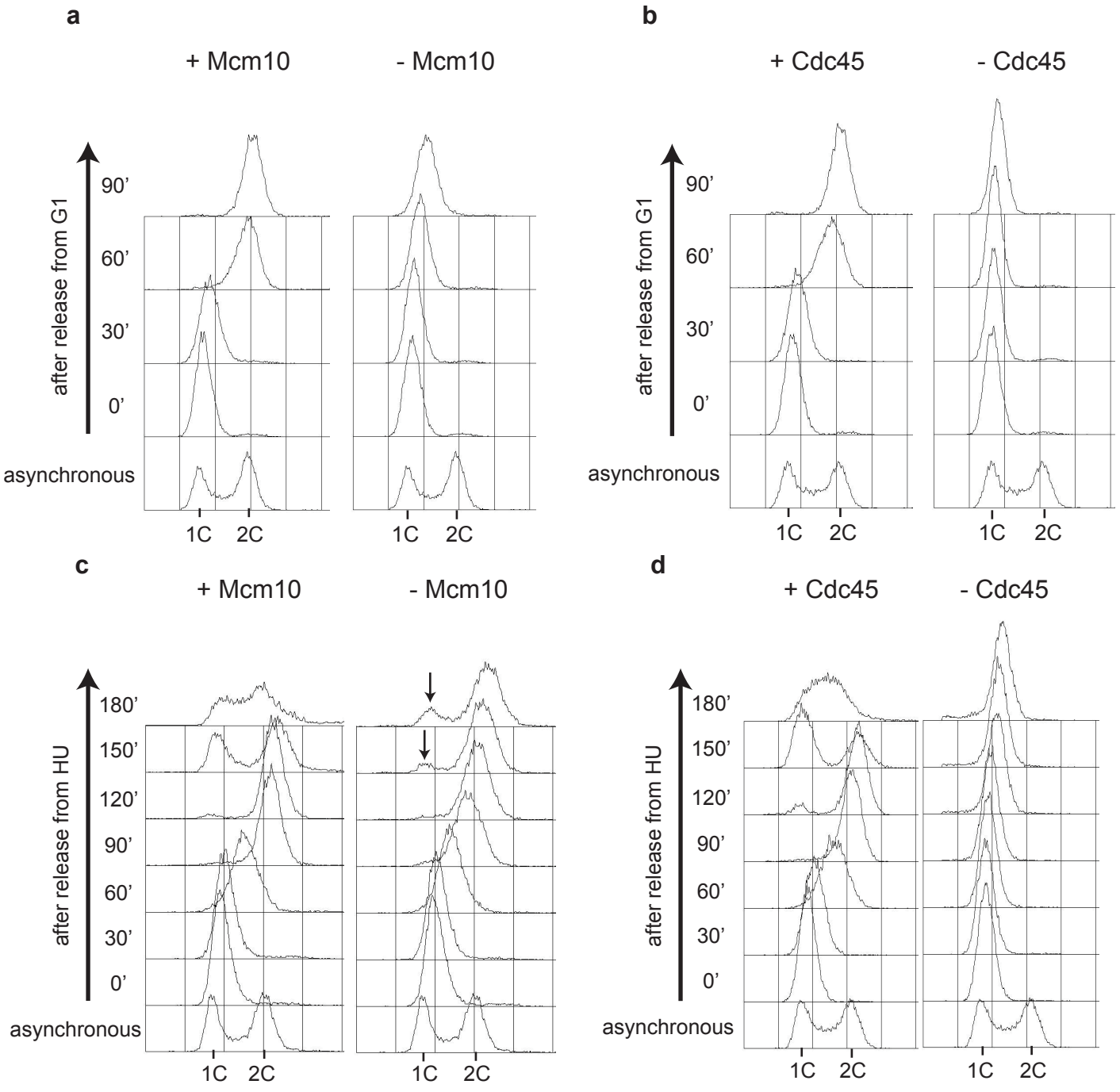
a
+ Mcm10
- Mcm10
after release from G1
90'
60'
30'
0'
asynchronous
1C
2C
b
+ Cdc45
- Cdc45
c
+ Mcm10
- Mcm10
after release from HU
180'
150'
120'
90'
60'
30'
0'
d
+ Cdc45
- Cdc45

Figure 6

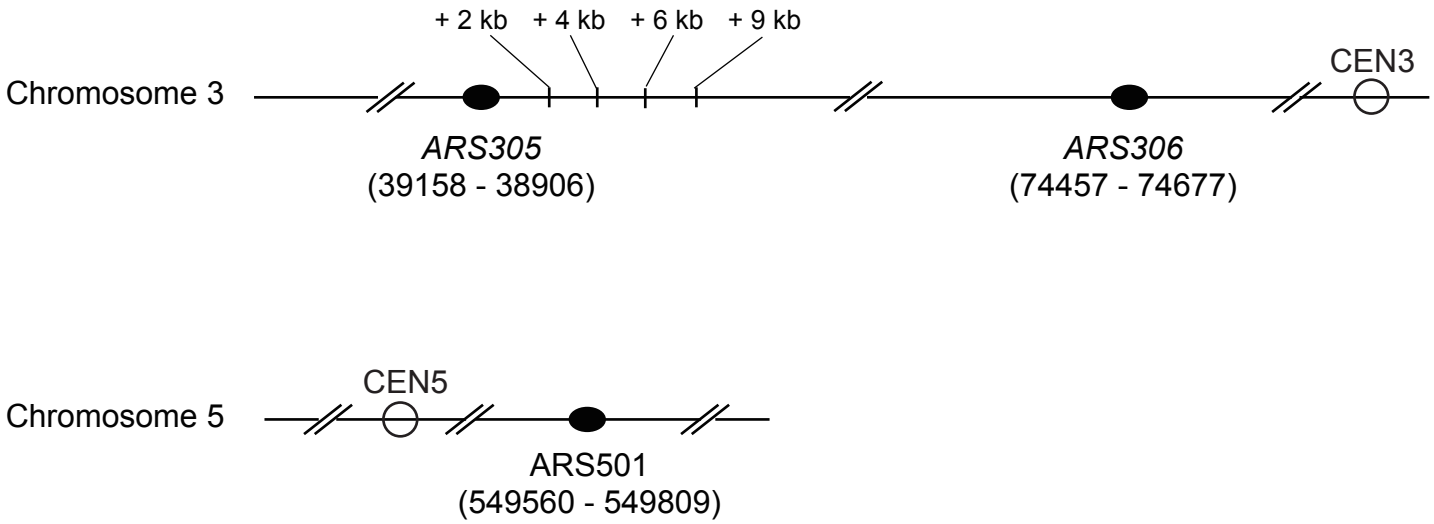
+ 2 kb
+ 4 kb
+ 6 kb
+ 9 kb
Chromosome 3
CEN3
ARS305
(39158 - 38906)
ARS306
(74457 - 74677)
CEN5
Chromosome 5
ARS501
(549560 - 549809)

Figure 7

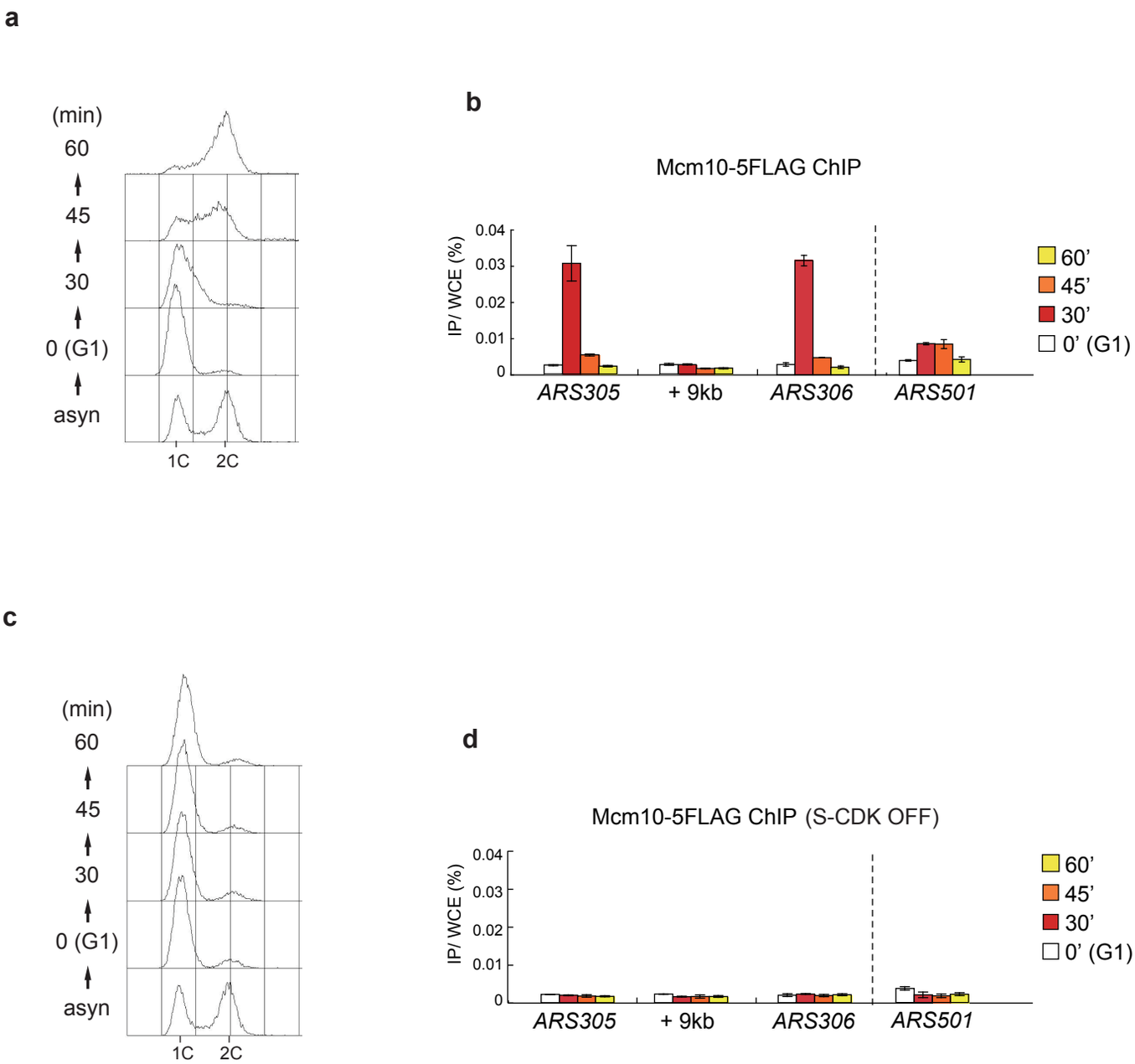
a
(min)
60
45
30
0 (G1)
asyn
1C
2C
b
Mcm10-5FLAG ChIP
IP/ WCE (%)
0.04
0.03
0.02
0.01
0
ARS305
+ 9kb
ARS306
ARS501
60'
45'
30'
0' (G1)
c
(min)
60
45
30
0 (G1)
asyn
1C
2C
d
Mcm10-5FLAG ChIP (S-CDK OFF)
IP/ WCE (%)
0.04
0.03
0.02
0.01
0
ARS305
+ 9kb
ARS306
ARS501
60'
45'
30'
0' (G1)

Figure 8

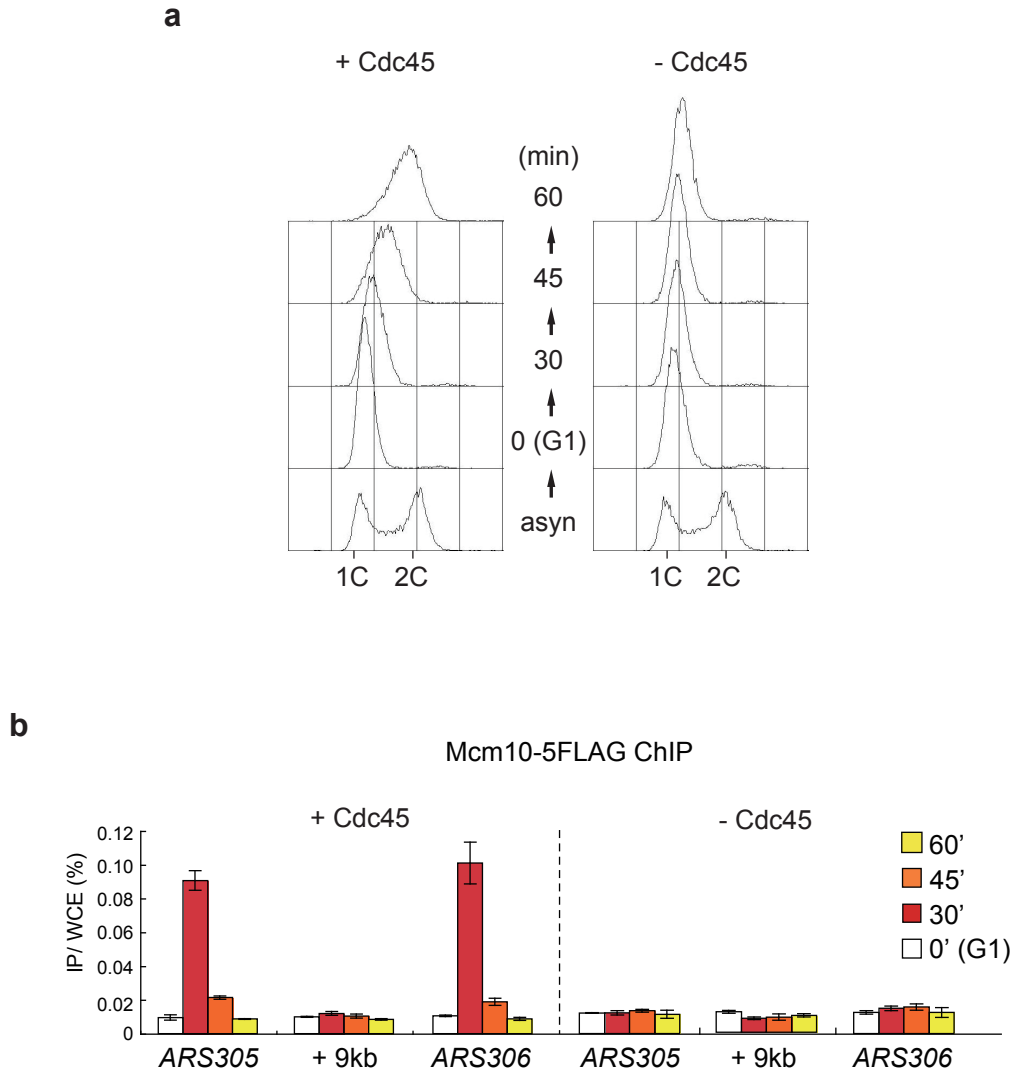
a
+ Cdc45
- Cdc45
(min)
60
45
30
0 (G1)
asyn
1C
2C
1C
2C
b
Mcm10-5FLAG ChIP
+ Cdc45
- Cdc45
IP/ WCE (%)
0.12
0.10
0.08
0.06
0.04
0.02
0
60'
45'
30'
0' (G1)
ARS305
+ 9kb
ARS306
ARS305
+ 9kb
ARS306

Figure 9

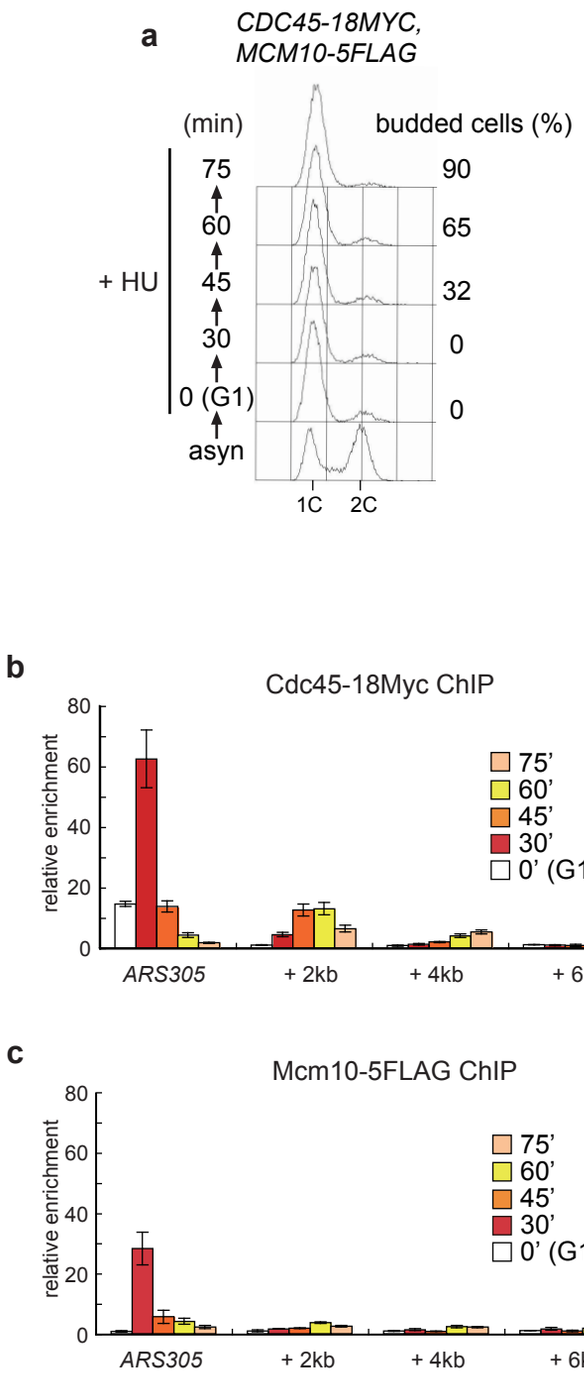
a
CDC45-18MYC,
MCM10-5FLAG
(min)
budded cells (%)
75
90
60
65
+ HU
45
32
30
0
0 (G1)
0
asyn
1C
2C
b
Cdc45-18Myc ChIP
relative enrichment
80
60
40
20
0
75'
60'
45'
30'
0' (G1)
ARS305
+ 2kb
+ 4kb
+ 6kb
c
Mcm10-5FLAG ChIP
relative enrichment
80
60
40
20
0
75'
60'
45'
30'
0' (G1)
ARS305
+ 2kb
+ 4kb
+ 6kb

Figure 10

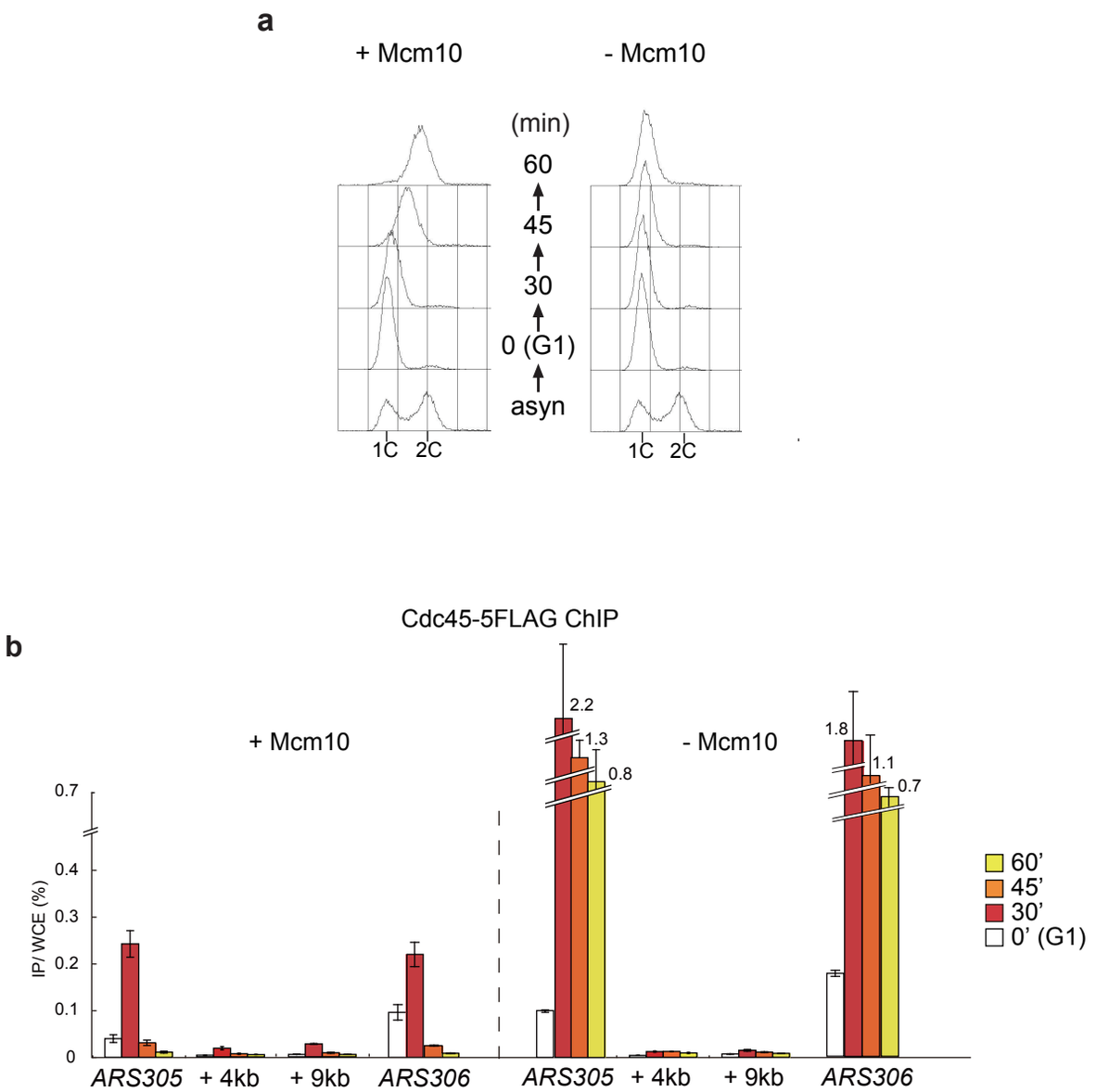
a
+ Mcm10
- Mcm10
(min)
60
45
30
0 (G1)
asyn
1C
2C
1C
2C
b
Cdc45-5FLAG ChIP
+ Mcm10
- Mcm10
IP/ WCE (%)
0.7
0.4
0.3
0.2
0.1
0
2.2
1.3
0.8
1.8
1.1
0.7
ARS305
+ 4kb
+ 9kb
ARS306
ARS305
+ 4kb
+ 9kb
ARS306
60'
45'
30'
0' (G1)

Figure 11

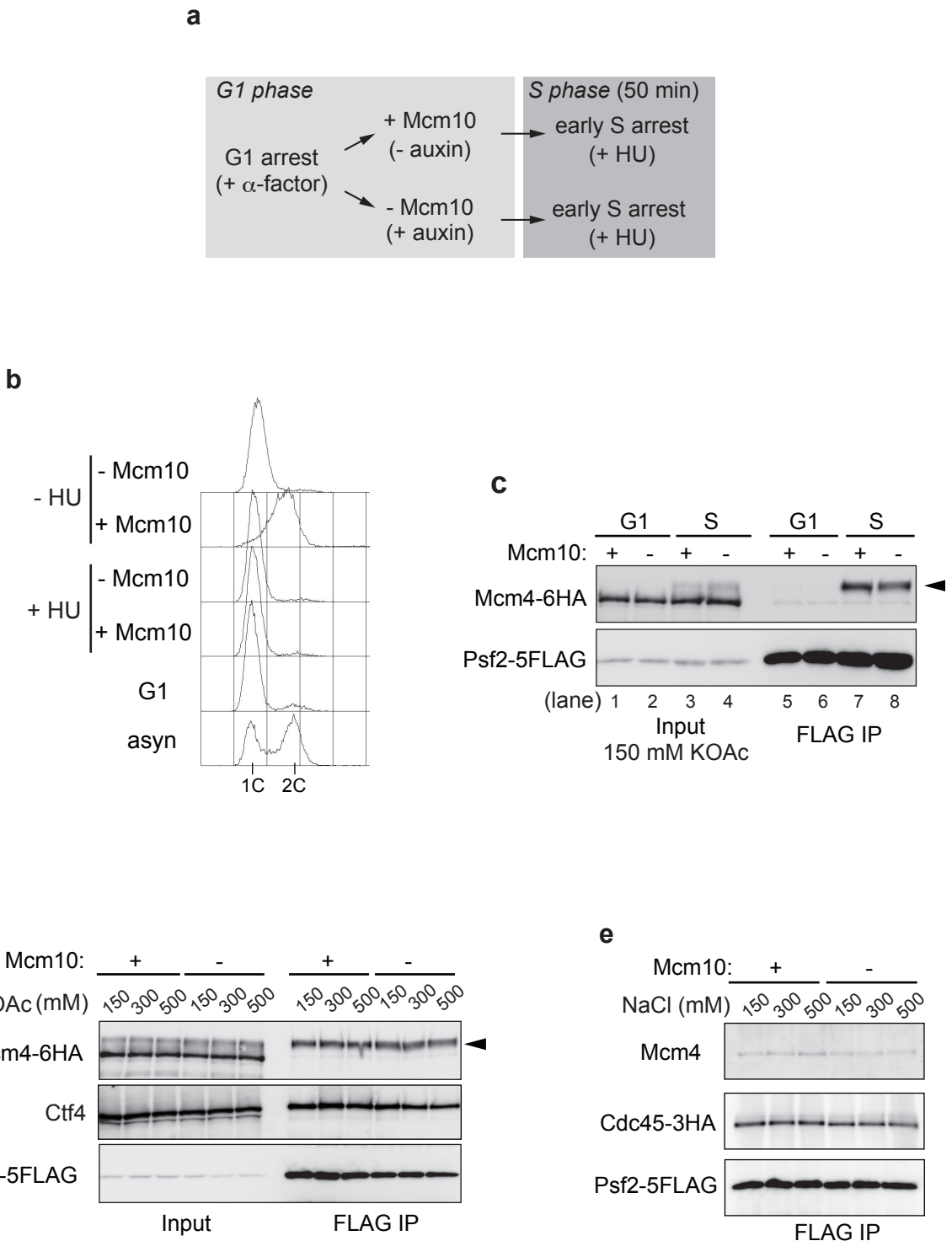
a
G1 phase
S phase (50 min)
G1 arrest
(+ α-factor)
+ Mcm10
(- auxin)
- Mcm10
(+ auxin)
early S arrest
(+ HU)
early S arrest
(+ HU)
b
- HU
+ HU
- Mcm10
+ Mcm10
- Mcm10
+ Mcm10
G1
asyn
1C
2C
c
G1
S
G1
S
Mcm10:
+ - + - + - + -
Mcm4-6HA
Psf2-5FLAG
(lane) 1 2 3 4 5 6 7 8
Input
150 mM KOAc
FLAG IP
d
Mcm10:
+
-
+
-
KOAc (mM)
150 300 500 150 300 500 150 300 500 150 300 500
Mcm4-6HA
Ctf4
Psf2-5FLAG
Input
FLAG IP
e
Mcm10:
+
-
NaCl (mM)
150 300 500 150 300 500
Mcm4
Cdc45-3HA
Psf2-5FLAG
FLAG IP

Figure 12

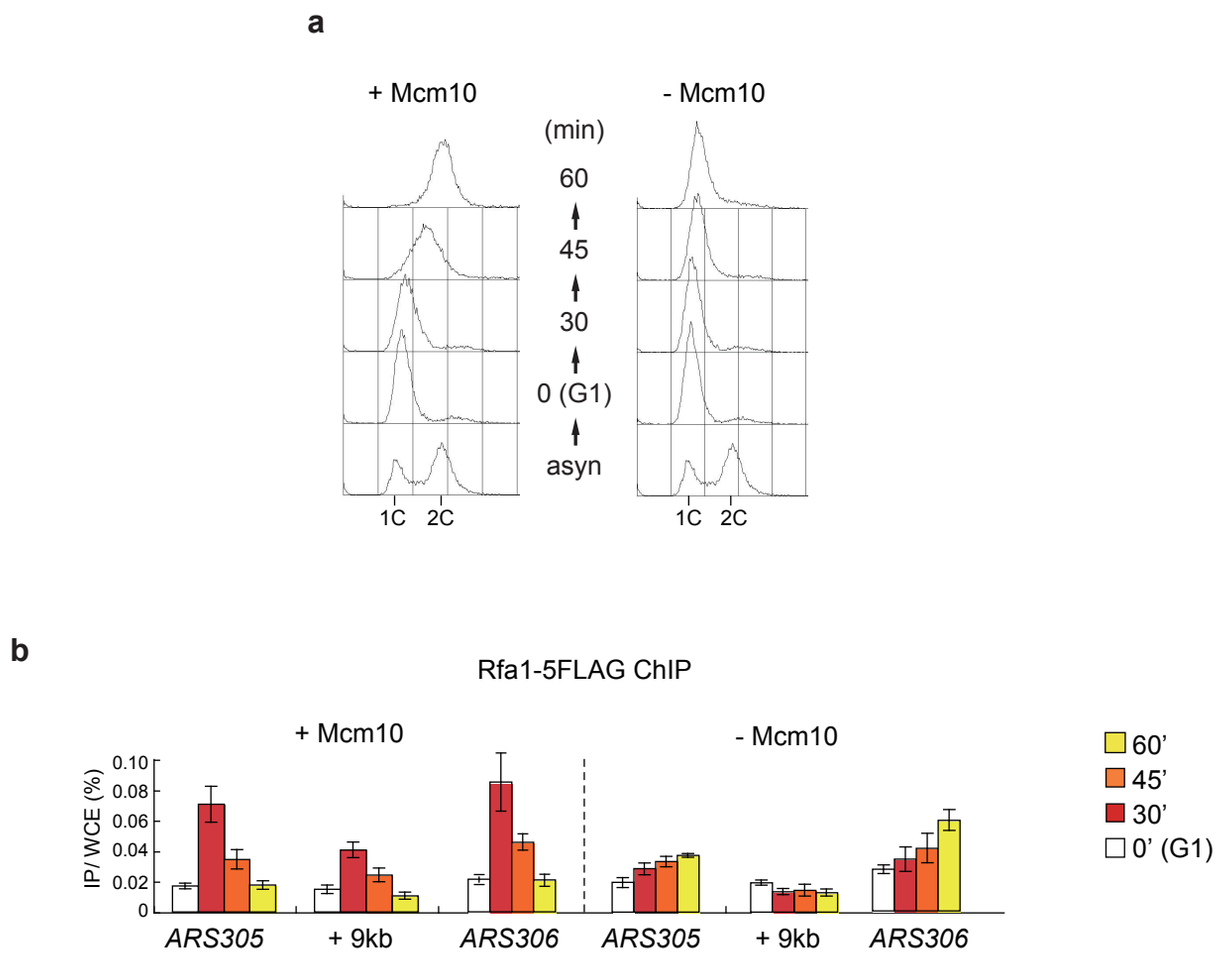
a
+ Mcm10
- Mcm10
(min)
60
45
30
0 (G1)
asyn
1C
2C
1C
2C
b
Rfa1-5FLAG ChIP
+ Mcm10
- Mcm10
IP/ WCE (%)
0.10
0.08
0.06
0.04
0.02
0
ARS305
+ 9kb
ARS306
ARS305
+ 9kb
ARS306
60'
45'
30'
0' (G1)

Figure 13

a

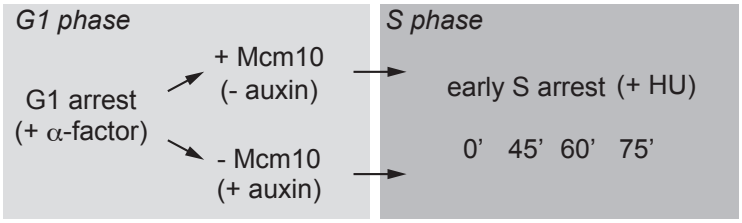

b

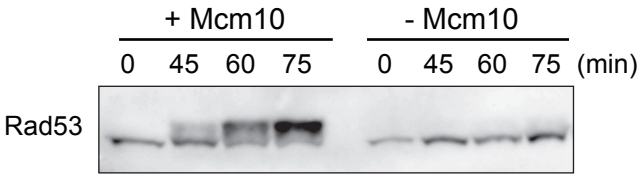

c

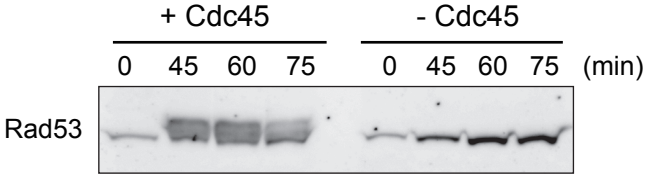

Figure 14

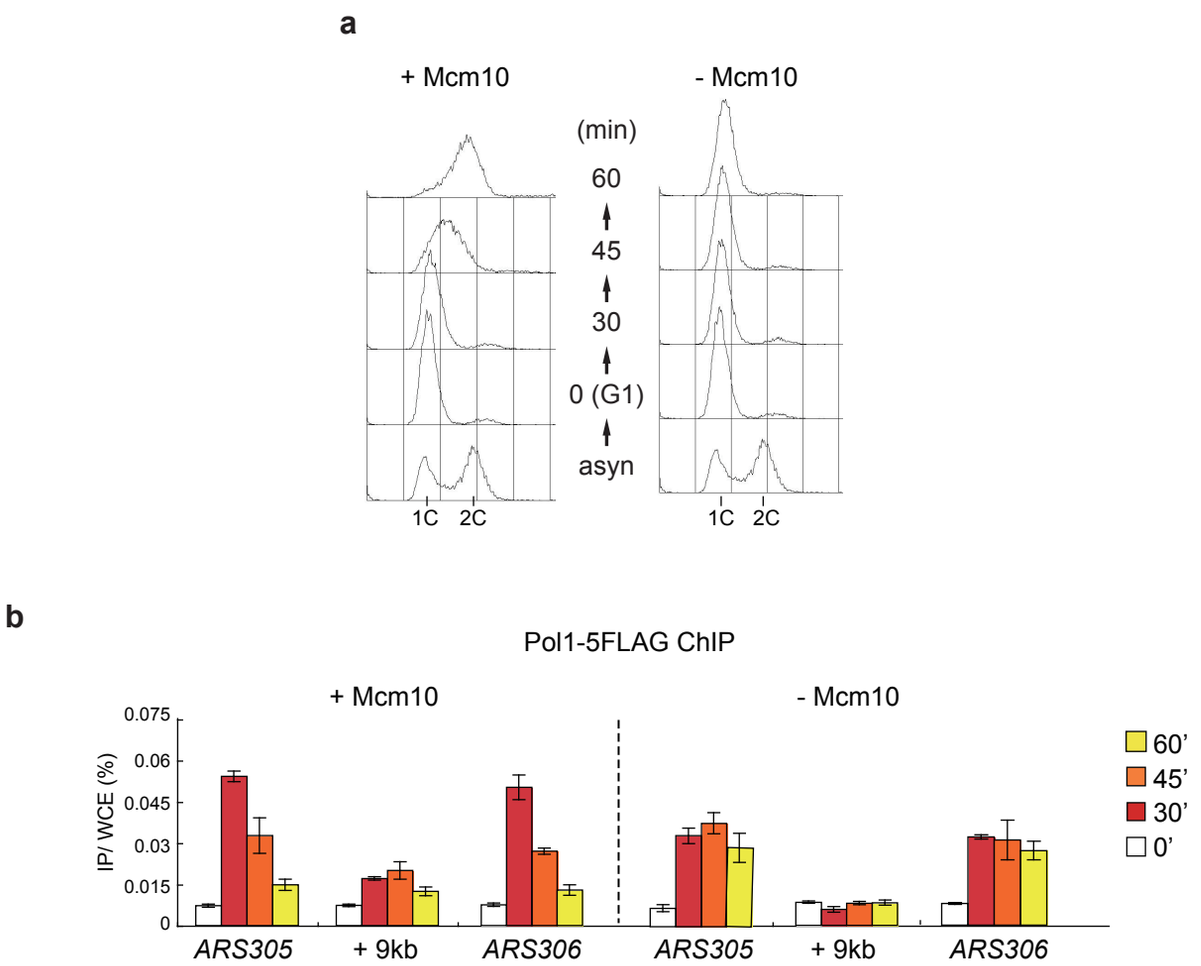
a
+ Mcm10
- Mcm10
(min)
60
45
30
0 (G1)
asyn
1C
2C
1C
2C
b
Pol1-5FLAG ChIP
+ Mcm10
- Mcm10
IP/ WCE (%)
0.075
0.06
0.045
0.03
0.015
0
60'
45'
30'
0'
ARS305
+ 9kb
ARS306
ARS305
+ 9kb
ARS306

Figure 15

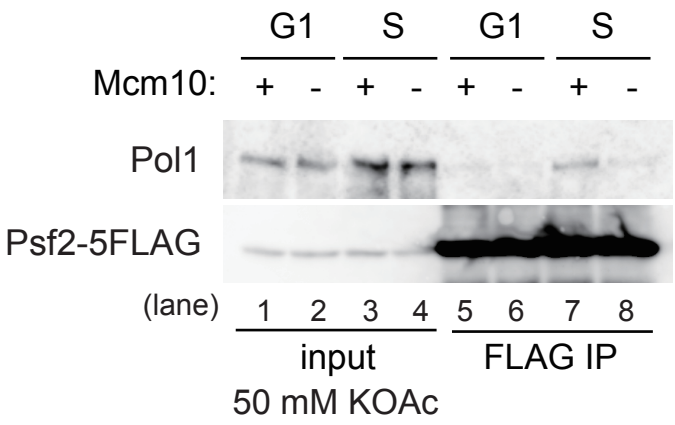
G1
S
G1
S
Mcm10:
+ - + - + - + -
Pol1
Psf2-5FLAG
(lane)
1 2 3 4 5 6 7 8
input
FLAG IP
50 mM KOAc

Figure 16

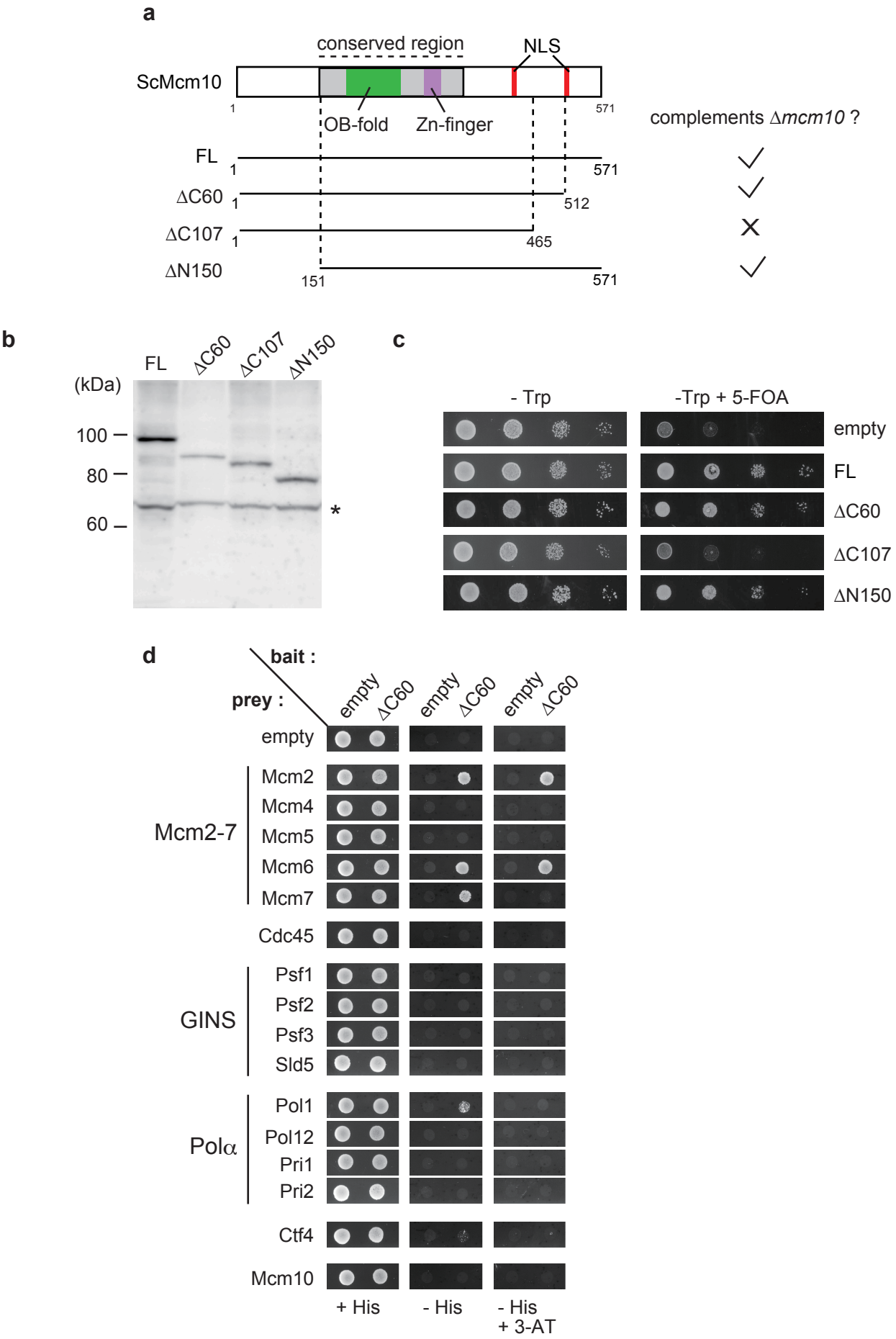
a
conserved region
NLS
ScMcm10
1
571
OB-fold
Zn-finger
complements Δmcm10 ?
FL
1
571
ΔC60
1
512
ΔC107
1
465
ΔN150
151
571
b
FL
ΔC60
ΔC107
ΔN150
(kDa)
100
80
60
*
c
- Trp
-Trp + 5-FOA
empty
FL
ΔC60
ΔC107
ΔN150
d
bait :
prey :
empty
ΔC60
Mcm2
Mcm4
Mcm5
Mcm6
Mcm7
Mcm2-7
Cdc45
Psf1
Psf2
Psf3
Sld5
GINS
Pol1
Pol12
Pri1
Pri2
Polα
Ctf4
Mcm10
+ His
- His
- His
+ 3-AT

Figure 17

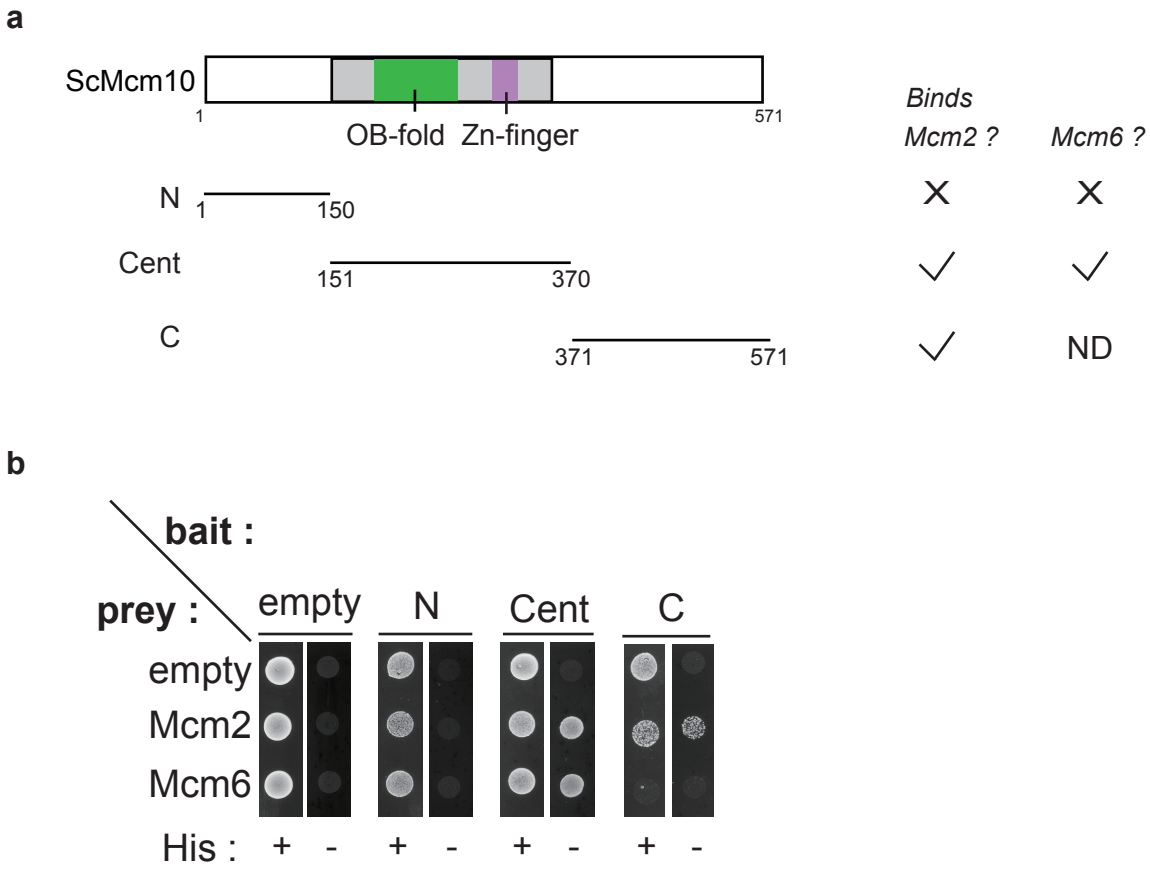
a
ScMcm10
1
571
OB-fold
Zn-finger
Binds
Mcm2 ?
Mcm6 ?
N
1
150
X
X
Cent
151
370
C
371
571
ND
b
bait :
prey :
empty
N
Cent
C
empty
Mcm2
Mcm6
His :
+ - + - + - + -

Figure 18

a

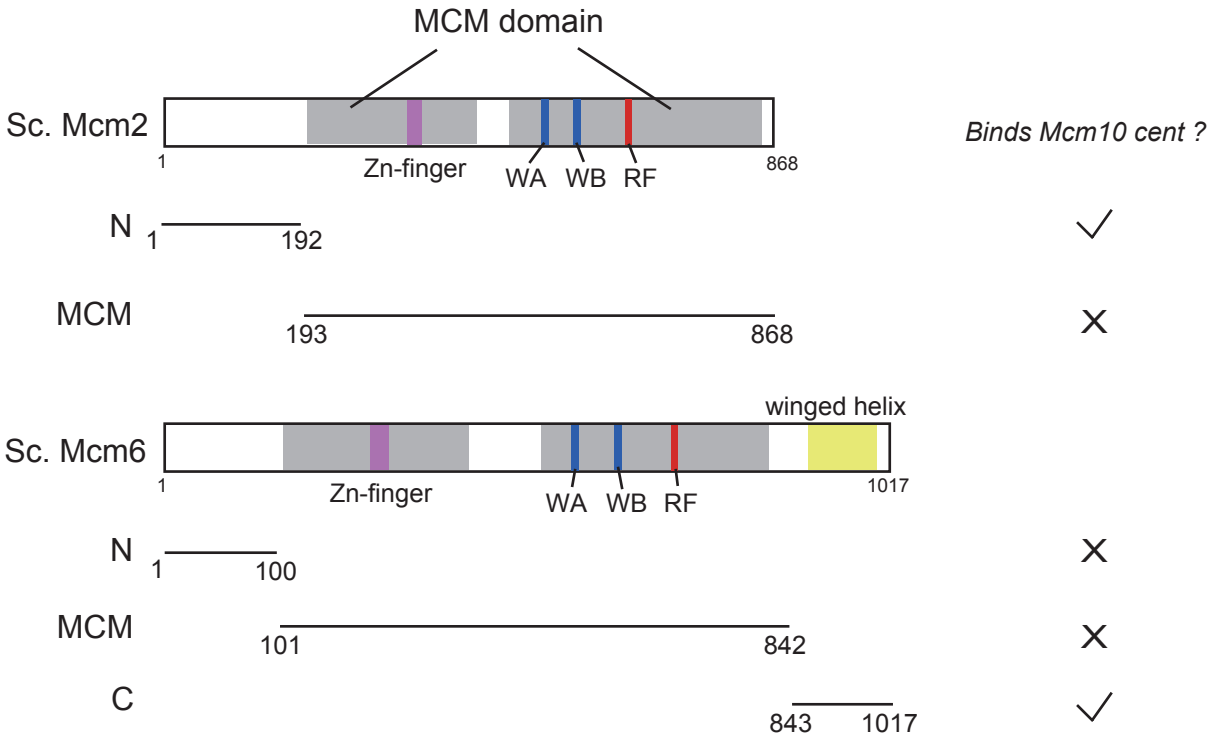
MCM domain
Sc. Mcm2
Binds Mcm10 cent ?
1
Zn-finger
WA
WB
RF
868
N
1
192
MCM
193
868
winged helix
Sc. Mcm6
1
Zn-finger
WA
WB
RF
1017
N
1
100
MCM
101
842
C
843
1017

b

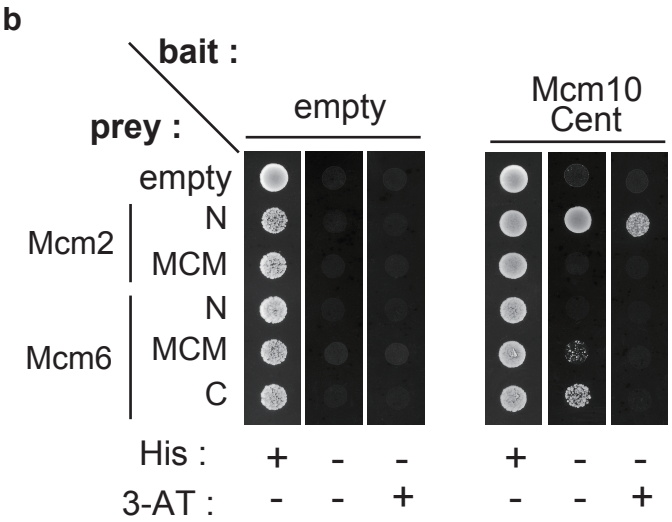
bait :
prey :
empty
Mcm10
Cent
empty
Mcm2
N
MCM
Mcm6
N
MCM
C
His :
3-AT :

Figure 19

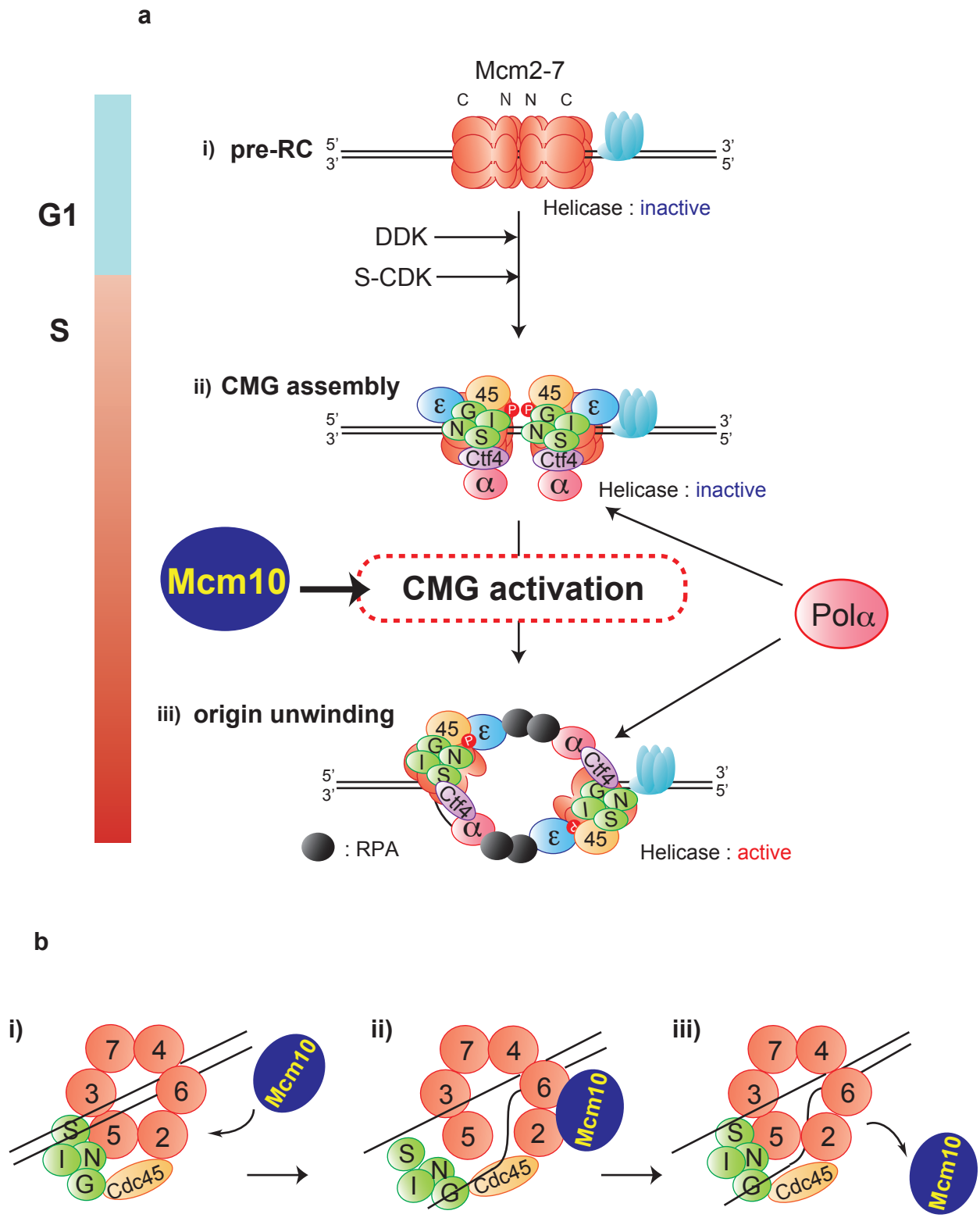
a
G1
S
Mcm2-7
C N N C
i) pre-RC
5'
3'
3'
5'
Helicase : inactive
DDK
S-CDK
ii) CMG assembly
45
ε
G
I
N
S
Ctf4
α
P
Helicase : inactive
Mcm10
CMG activation
Polα
iii) origin unwinding
: RPA
Helicase : active
b
i)
ii)
iii)
7
4
3
6
5
2
S
I
N
G
Cdc45
Mcm10

Figure 20

Table 1 The controversy of reported roles of Mcm10

Organism: / Reported role:	budding yeast	fission yeast	frog	human
Required for loading of Cdc45 ?	**YES** (Sawyer et al., 2004) **NO** (Heller et al., 2011)	**YES** (Gregan et al., 2003)	**YES** (Whohlschlegel et al., 2002)	
Required for Polα stability ?	**YES** (Ricke and Bielinsky, 2004) **NO** (Heller et al., 2011)			**YES** (Chattopadhyway and Bielinsky, 2007) **NO** (Zhu et al., 2007)

Table 2 Strains used in this study

Strain	Genotype	Source
W303-1a	*MATa ade2-1 ura3-1 his3-11,15 trp1-1 leu2-3,112 can1-100*	R. Rothstein
W303-1b	*MATα ade2-1 ura3-1 his3-11,15 trp1-1 leu2-3,112 can1-100*	R. Rothstein
BTY100	*MATa mcm10-1 (P269L)*	Kawasaki et al.
YNK40	*MATa ura3-1::GAL-OsTIR1-9MYC (URA3)*	Nishimura et al.
YNK91	*MATa ura3-1::GAL-OsTIR1-9MYC (URA3) cdc45::cdc45-aid (KanMX)*	Nishimura et al.
YJW18	*MATa mcm10::mcm10-aid (KanMX)*	This study
YJW19	*MATa mcm10::mcm10-1-aid (KanMX)*	This study
YNK43	*MATα ura3-1::GAL-OsTIR1-9MYC (URA3)*	Lab stock
YLD12	*MATa ura3-1::GAL-SIC1ΔNT (URA3)*	Lab stock
YJW30	*MATa mcm10::MCM10-5FLAG (HIS3)*	This study
YJW31	*MATα mcm10::MCM10-5FLAG (HIS3)*	This study ***1**
YMK369	*MATa cdc45::CDC45-18MYC (k.l.TRP1)*	Kanemaki et al. (2006)
YMK398	*MATa cdc45::CDC45-5FLAG (hphNT)*	Lab stock
YJW48	*MATα cdc45::CDC45-5FLAG (hphNT)*	This study ***2**
YJW82	*MATa ura3-1::GAL-OsTIR1-9MYC (URA3) mcm10::mcm10-aid (KanMX)*	This study ***3**
YJW50	*MATa ura3-1::GAL-OsTIR1-9MYC (URA3) mcm10::mcm10-1-aid (KanMX)*	This study ***4**
YJW52	*MATa ura3-1::GAL-SIC1ΔNT (URA3) mcm10::MCM10-5FLAG (HIS3)*	This study ***5**
YJW54	*MATa mcm10::MCM10-5FLAG (HIS3) cdc45::CDC45-18MYC (k.l.TRP1)*	This study ***6**
YJW60	*MATa ura3-1::GAL-OsTIR1-9MYC (URA3) mcm10::mcm10-1-aid (KanMX) cdc45::CDC45-5FLAG (hphNT)*	This study ***7**
YJW65	*MATa ura3-1::GAL-OsTIR1-9MYC (URA3) cdc45::cdc45-aid (KanMX) mcm10::MCM10-5FLAG (HIS3)*	This study ***8**
YJW90	*MATα ura3-1::GAL-OsTIR1-9MYC (URA3) rfa1::RFA1-5FLAG (HIS3)*	This study
YJW97	*MATa ura3-1::GAL-OsTIR1-9MYC (URA3) mcm10::mcm10-1-aid (KanMX) rfa1::RFA1-5FLAG (HIS3)*	This study ***9**
YJW64	*MATα ura3-1::GAL-OsTIR1-9MYC (URA3) pol1::POL1-5FLAG (HIS3)*	This study
YJW112	*MATa ura3-1::GAL-OsTIR1-9MYC (URA3) mcm10::mcm10-1-aid (KanMX) pol1::POL1-5FLAG (HIS3)*	This study ***10**
YNK102	*MATα psf2::PSF2-5FLAG (hphNT)*	Lab stock
YJW106	*MATα ura3-1::GAL-OsTIR1-9MYC (URA3) mcm10::mcm10-1-aid (KanMX) psf2::PSF2-5FLAG (hphNT)*	This study ***11**
YMK714	*MATa ura3-1::GAL-OsTIR1-9MYC (URA3) mcm4::MCM4-6HA (k.l.TRP1)*	Lab stock

YJW184	*MATa ura3-1::GAL-OsTIR1-9MYC (URA3)* *mcm10::mcm10-1-aid (KanMX)* *psf2::PSF2-5FLAG (hphNT) mcm4::MCM4-6HA (k.l.TRP1)*	This study ***12**
YMK283	*MATa cdc45::CDC45-3HA (k.l.TRP1)*	Lab stock
YJW193	*MATa ura3-1::GAL-OsTIR1-9MYC (URA3)* *mcm10::mcm10-1-aid (KanMX)* *psf2::PSF2-5FLAG (hphNT) cdc45::CDC45-3HA (k.l.TRP1)*	This study ***13**
YJW156	*MATa/α MCM10/mcm10::Δmcm10 (hphNT)*	This study
YJW158	*MATa mcm10::mcm10Δ (hphNT) pRS316-pMcm10-MCM10 (URA3)*	This study
YJW202	*MATa mcm10::mcm10Δ (hphNT) pRS316-pMcm10-MCM10 (URA3)* *pRS414-pMcm10-GFP-NLS (TRP1)*	This study
YJW203	*MATa mcm10::mcm10Δ (hphNT) pRS316-pMcm10-MCM10 (URA3)* *pRS414-pMcm10-MCM10-GFP-NLS (TRP1)*	This study
YJW205	*MATa mcm10::mcm10Δ (hphNT) pRS316-pMcm10-MCM10 (URA3)* *pRS414-pMcm10-mcm10ΔC60 (1-512) -GFP-NLS (TRP1)*	This study
YJW206	*MATa mcm10Δ::hphNT pRS316-pMcm10-MCM10 (URA3)* *pRS414-pMcm10-mcm10ΔC107 (1-465) -GFP-NLS (TRP1)*	This study
L40	*MATa his3-delta200 trp1-901 leu2-3112 ade2 lys2-801am* *LYS2::(lexAop)4-HIS3* *URA3::(lexAop)8-lacZ GAL4*	Gifted from S. Mimura

W303 is the parental strain for all the others, except for L40 strain

*1 YJW31 was derived from same tetrad analysis when YJW30 was obtained

*2 YJW48 was obtained by back crossing YMK398 with W303-1b

*3 YMK82 was obtained by crossing YNK43 with YJW18

*4 YJW50 was obtained by crossing YNK43 with YJW19

*5 YJW52 was obtained by crossing YLD12 with YJW31

*6 YJW54 was obtained by crossing YMK369 with YJW31

*7 YJW60 was obtained by crossing YJW50 with YJW48

*8 YJW65 was obtained by crossing YNK91 with YJW31

*9 YJW97 was obtained by crossing YJW50 with YJW90

*10 YJW112 was obtained by crossing YJW50 with YJW64

*11 YJW106 was obtained by crossing YJW50 with YNK102

*12 YJW184 was obtained by crossing YJW106 with YMK714

*13 YJW193 was obtained by crossing YJW106 with YMK283

Table 3 Oligos used in this study

No.	Oligo	Sequence	used for
1	ARS305 5'	AGCCTTCTTTGGAGCTCAAGTG	ChIP-qPCR
2	ARS305 3'	TTTGAGGAATTTCTTTTGAAGAGTTG	ChIP-qPCR
3	ARS305+2kb 5'	CGATAACGGCTAAAACAATTAAAGC	ChIP-qPCR
4	ARS305+2kb 3'	GCTAGAACAGCGACAATGTTTTTG	ChIP-qPCR
5	ARS305+4kb 5'	GGTACAATCATAGAAAAAGGGTACAAAGA	ChIP-qPCR
6	ARS305+4kb 3'	GGATTTGCTGAGTTCGCGTATT	ChIP-qPCR
7	ARS305+6kb 5'	TGTTCTTCATTAGCGATCAGATAAGC	ChIP-qPCR
8	ARS305+6kb 3'	AAACAACAAACCTAAACACTCTTGGTATT	ChIP-qPCR
9	ARS305+9kb 5'	AACTTGGCCTTATGTAGAATTTCTTGA	ChIP-qPCR
10	ARS305+9kb 3'	AGCAATTCCACCGACCATACTC	ChIP-qPCR
11	ARS306 5'	CGTCTAAGTCCTTGTAATGTAAGGTAAGAA	ChIP-qPCR
12	ARS306 3'	GCTTGGGTTTGTGACTTACTAACG	ChIP-qPCR
13	ARS501 5'	CTCATCATCATCCCCGGTAAA	ChIP-qPCR
14	ARS501 3'	CGTACACTAGCCCGTTGAGGTAT	ChIP-qPCR
15	ApaI-Mcm10 1 5'	ACGTCAGGGCCCATGAATGATCCTCGTGAAAT	plasmid shuffle assay
16	ApaI-Mcm10 151 5'	ACGTCAGGGCCCATGCCGATAATCACAAACGAATT	plasmid shuffle assay
17	Mcm10 465-ApaI 3'	ACGTCAGGGCCCCTGTCGCTCTCCGACGCTCT	plasmid shuffle assay
18	Mcm10 571-ApaI 3'	ACGTCAGGGCCCTATTATCTCAAGATCGCTGG	plasmid shuffle assay
19	Mcm10 512-ApaI 3'	ACGTCAGGGCCCTTTACCGAGTAAGTTGTTCT	plasmid shuffle assay
20	EcoRI-Mcm10 1 5'	ATCGATGAATTCATGAATGATCCTCGTGAAATTTT	yeast two-hybrid assay
22	Mcm10 512-SalI 3'	ATCGATGTCGACTTTACCGAGTAAGTTGTTCTTAG	yeast two-hybrid assay
23	EcoRI-Mcm10 151 5'	ATCGATGAATTCCCGATAATCACAAACGAATTAG	yeast two-hybrid assay
24	EcoRI-Mcm10 371 5'	ATCGATGAATTCGCCAAAGGGGAAAACGGGTTTAATATAATC	yeast two-hybrid assay
25	Mcm10 150-SalI 3'	ATCGATGTCGACCACATATTTCTTCTCATCGGTAC	yeast two-hybrid assay
26	Mcm10 370-SalI 3'	ATCGATGTCGACCTTATATAGGCTTGGTTGAGAG	yeast two-hybrid assay
27	Mcm10 571-SalI 3'	ATCGATGTCGACTTATATTATCTCAAGATCGCTGG	yeast two-hybrid assay
28	AscI-A-Mcm2 1 5'	TGAGGCGCGCCAATGTCTGATAATAGAAGACGTAG	yeast two-hybrid assay
29	Mcm2 192-NotI 3'	TGAGGAGCGGCCGCGTTAGCCTTAACGTTACTCAG	yeast two-hybrid assay
30	AscI-A-Mcm2 193 5'	TGAGGCGCGCCAAGTTACTCGGAATGGATAACACAACC	yeast two-hybrid assay
31	Mcm2 868-NotI 3'	TGAGGAGCGGCCGCTTAGTGACCCAAGGTATAAATTGC	yeast two-hybrid assay
32	AscI-A-Mcm6 1 5'	TGAGGCGCGCCAATGTCATCCCCTTTTCCAGCTG	yeast two-hybrid assay
33	Mcm6 100-NotI 3'	TGAGGAGCGGCCGCAACGTGATTCAAAGCTCTAC	yeast two-hybrid assay
34	AscI-A-Mcm6 101 5'	TGAGGCGCGCCAAAGAAAGTTGATGACGTTACTGG	yeast two-hybrid assay
35	Mcm6 842-NotI 3'	TGAGGAGCGGCCGCATCATCCACATCAACACGAATAATAC	yeast two-hybrid assay
36	AscI-A-Mcm6 843 5'	TGAGGCGCGCCAGTGGAAATGGATGAAGAATTTG	yeast two-hybrid assay
37	Mcm6 1017-NotI 3'	TGAGGAGCGGCCGCTTAGCTGGAATCCTGTGGTTC	yeast two-hybrid assay
38	AscI-A-Mcm7 1 5'	TGAGGCGCGCCAATGAGTGCGGCACTTCCATCAATTC	yeast two-hybrid assay
39	Mcm7 730-NotI 3'	TGAGGAGCGGCCGCTTCTTGATACAATGATTCCTTGG	yeast two-hybrid assay
40	AscI-A-Mcm7 731 5'	TGAGGCGCGCCAACCAACAAATCTAAAGAAGATG	yeast two-hybrid assay
41	Mcm7 845-NotI 3'	TGAGGAGCGGCCGCTCAAGCGTCTTGTAGATCGATATC	yeast two-hybrid assay
42	Mcm10 C-tagging 5'	AGGAAACTAAAGAAACTTCTGACGGTAGTGCCAGCGATCTTGAG ATAATACGTACGCTGCAGGTCGAC	tagging to C-terminus of endogenous Mcm10
43	Mcm10 C-tagging 3'	TTCTTTCTCACTTTAAGGATTGATTCCCTATATTGCAACCAAAAT CACTCATCGATGAATTCGAGCTCG	tagging to C-terminus of endogenous Mcm10
44	Mcm10 C-check 5'	AATAGTAATTCTGCCAAAGC	checking tagging to C-terminus of Mcm10
45	Mcm10 C-check 3'	ATCTACAATTCCAGGCACCC	checking tagging to C-terminus of Mcm10

46	KanMX forward	CAAGAACTTGTCATTTGTATAG	checking selection marker is inserted
47	KanMX reverse	GAACCTCAGTGGCAAATCC	checking selection marker is inserted
48	HIS3MX forward	TATTGTCCACTTGACGAAGC	checking selection marker is inserted
49	HIS3MX reverse	CAGTGTGATGATCATCGATG	checking selection marker is inserted
50	Rfa1 tagging 5'	GGGCTGAAGCCGACTATCTTGCCGATGAGTTATCCAAGGCT TTGTTAGCTCGTACGCTGCAGGTCGAC	tagging to C-terminus of endogenous Rfa1
51	Rfa1 tagging 3'	TCCAGTCATCAAGAGATGCTGAACCGCCCTTCAAAAACTTG ACGAAATAGATCGATGAATTCGAGCTCG	tagging to C-terminus of endogenous Rfa1
52	Rfa1 Check 5'	TATTGCTAGAGCTCAAGCTG	checking tagging to C-terminus of Rfa1
53	Rfa1 Check 3'	ACGGTTCACAATCCCTACAG	checking tagging to C-terminus of Rfa1
54	Pol1 tagging 5'	GTGGACGTCGCTACGTTGATATGACTAGCATATTTGATTTCATG CTAAATCGTACGCTGCAGGTCGAC	tagging to C-terminus of endogenous Pol1
55	Pol1 tagging 3'	TCCGATGTCTGTACATTAGGTATCTAGTAGGATGCGTATGTACA GTTGTAATCGATGAATTCGAGCTCG	tagging to C-terminus of endogenous Pol1
56	Pol1 Check 5'	TGACAAGCAATTGTACAATC	checking tagging to C-terminus of Pol1
57	Pol1 Check 3'	TCTTGCTGATAAGGCGAATC	checking tagging to C-terminus of Pol1
58	Mcm10 N-tagging 5'	AGAAATATCAACTTTATAGGCCATCGAAGATAAAGGAACGTA AGTTTGTCATTAAGGCGCGCCAGATCTG	tagging to N-terminus of endogenous Mcm10
59	Mcm10 N-check 5'	CGTACACTCAATATTCAACC	checking tagging to N-terminus of Mcm10
60	hphNT forward	CATATGCGCGATTGCTGATC	checking selection marker is inserted
61	hphNT reverse	AATAGGTCAGGCTCTCGCTG	checking selection marker is inserted
62	Mcm10 cloning 5'	AACCGGAATTCAATATTCAACCTGAAGTTGCAGTC	cloning *MCM10* ORF and its promoter region
63	Mcm10 cloning 3'	ACCGGACCCGGGTCTTGTTGTTATGTATTGAACC	cloning *MCM10* ORF and its promoter region
64	Mcm10 promoter 5'	ATCGAGAATTCAATATTCAACCTGAAG	cloning native *MCM10* promoter region
65	Mcm10 promoter 3'	TACTGAGGGCCCTTCTCCACGAACCAAGTGCT	cloning native *MCM10* promoter region

Table 4 Plasmids used in this study

Plasmid	Construct	Source
pJW3	pRS316/ *MCM10 promoter-MCM10*	This study
pJW4	pRS414/ *GFP-NLS*	This study
pJW5	pRS414/ *MCM10 promoter-GFP-NLS*	This study
pJW6	pRS414/ *MCM10 promoter-MCM10-GFP-NLS*	This study
pJW8	pRS414/ *MCM10 promoter-mcm10Δ107 (1-465)-GFP-NLS*	This study
pJW12	pRS414/ *MCM10 promoter-mcm10ΔC60 (1-512)-GFP-NLS*	This study
pJW7	pRS414/ *MCM10 promoter-mcm10ΔN150 (151-571)-GFP-NLS*	This study
pSM378	*NLS-B42-HA-CTF4*	Mimura et al., 2009
pSM559	*NLS-B42-HA*	Mimura et al., 2010
pNYN20	*NLS-B42-HA-SLD5*	Y. Nakajima and S. Mimura, unpublished
pNYN31	*NLS-B42-HA-MCM7*	Y. Nakajima and S. Mimura, unpublished
pNYN22	*NLS-B42-HA-MCM4*	Y. Nakajima and S. Mimura, unpublished
pNYN23	*NLS-B42-HA-MCM5*	Y. Nakajima and S. Mimura, unpublished
pNYN25	*NLS-B42-HA-POL12*	Y. Nakajima and S. Mimura, unpublished
pNYN31	*NLS-B42-HA-MCM7*	Y. Nakajima and S. Mimura, unpublished
pNYN32	*NLS-B42-HA-MCM10*	Y. Nakajima and S. Mimura, unpublished
pSM671	*LexABD-NLS*	Y. Nakajima and S. Mimura, unpublished
pNYN16	*NLS-B42-HA-CDC45*	Y. Nakajima and S. Mimura, unpublished
pNYN18	*NLS-B42-HA-PSF1*	Y. Nakajima and S. Mimura, unpublished
pNYN19	*NLS-B42-HA-PSF2*	Y. Nakajima and S. Mimura, unpublished
pNYN24	*NLS-B42-HA-POL1*	Y. Nakajima and S. Mimura, unpublished
pNYN26	*NLS-B42-HA-PRI1*	Y. Nakajima and S. Mimura, unpublished
pNYN27	*NLS-B42-HA-PRI2*	Y. Nakajima and S. Mimura, unpublished
pNYN29	*NLS-B42-HA-PSF3*	Y. Nakajima and S. Mimura, unpublished
pNYN30	*NLS-B42-HA-MCM6*	Y. Nakajima and S. Mimura, unpublished
pSM379	*NLS-B42-HA-MCM2*	Y. Nakajima and S. Mimura, unpublished
pJW29	*LexABD-mcm10ΔC60 (1-512) -NLS*	This study
pJW40	*LexABD-mcm10 N (1-150) -NLS*	This study
pJW41	*LexABD-mcm10 central (151-370) -NLS*	This study
pJW44	*LexABD-mcm10 C (371-571) -NLS*	This study
pJW45	*NLS-B42-HA-mcm2 N (1-192)*	This study
pJW46	*NLS-B42-HA-mcm2 MCM (193-868)*	This study
pJW47	*NLS-B42-HA-mcm6 N (1-100)*	This study
pJW48	*NLS-B42-HA-mcm6 MCM (101-842)*	This study
pJW49	*NLS-B42-HA-mcm6 C (843-1017)*	This study
pMK43	*aid-KanMX*	Nishimura et al
pKL259	*5FLAG-HIS3MX*	Gifted from Labib Lab
pNHK12	*aid-GFP-3NLS*	Nishimura et al

Figure legends

Figure 1

Overview of chromosomal DNA replication in eukaryotes. Multiple replication origins are distributed on one chromosome, including early-, late-, and dormant-origin (G1). Replication origins are activated in DDK and CDK dependent manner in S phase. Some origins are activated in early S phase (early origin; Early S), and others in late S phase (late origin; Late S). Dormant origin is not activated in normal S phase. Once bi-directional replication forks are established at activated origins, forks move away from the origins and whole chromosomal DNA is replicated (G2).

Figure 2

Initiation of DNA replication in budding yeast. (a) ORC binds to replication origins. (b) Formation of pre-RC. (c) Mcm2-7 is phosphorylated by DDK and that promotes association of Sld3-Cdc45 with replication origins. (d) S-CDK phosphorylates Sld2 and Sld3, and promotes pre-LC formation. (e) The CMG complex is assembled. (f) Start of DNA synthesis after priming short DNA, shown in red line, by Polα. (g) Polε synthesizes leading strand and Polδ does lagging strand. Serial and non-serial red lines show a leading and lagging strands, respectively.

Figure 3

Principle of auxin-inducible degron (AID) system. In plant, plant hormone auxin promotes the interaction of transcription repressors AUX/IAA with an auxin receptor TIR1. TIR1 is one component of SCF complex, which is an E3 ubiquitin ligase. As a result, AUX/IAA is polyubiquitinized and degraded by proteasome in auxin-dependent manner. SCF components, except for TIR1, are highly conserved among all eukaryotes. By expressing TIR1 in budding yeast, therefore, SCF^{TIR1} can be formed using the other endogenous components. Under this condition, a protein fused with AUX/IAA as the aid tag can be induced for degradation in the presence of auxin.

Figure 4

The *mcm10-1-aid* cells exhibit a pronounced defect in DNA replication. (a), Cell growth on plates. Serially diluted the *mcm10-1*, *mcm10-aid* (YJW82; *mcm10-aid, GAL-OsTIR1-9Myc), mcm10-1-aid* (YJW50; *mcm10-1-aid, GAL-OsTIR1-9Myc*), *cdc45-aid* (YNK91; *cdc45-aid, GAL-OsTIR1-9Myc*) or control (YNK40; *GAL-OsTIR1-9Myc*) cells were spotted and grown on a YPG plate under either permissive or non-permissive conditions as indicated in the figure. Plates were incubated for 3 days at 24°C except for *mcm10-1,* which was incubated at 37°C. (**b**), Flow cytometry analysis of *mcm10-1* and *mcm10-1-aid*. Yeast strains used in **a** were initially grown in YPR at 24°C before transfer to YPG at 24°C for 1 h. Afterwards, the cells were grown under the appropriate non-permissive conditions (37°C or 24°C with 500 μM IAA [indole-3-acetic acid; auxin]) to withdraw samples at indicated time points

and subjected to flow cytometry. (**c**), Immunoblotting to see the protein levels of Mcm10 and Mcm10-1-aid. Protein extracts prepared at 0 and 30 min from the wild-type and *mcm10-1-aid* cells grown as in Figure 4b were separated in SDS-polyacrylamide gel, transferred to a membrane, and blotted with anti-Mcm10 polyclonal antibody. Asterisk indicates a background protein. Ponceau staining of the membrane is shown as a loading control.

Figure 5

Polα is not affected after Mcm10 depletion in the *mcm10-1-aid* strain. Immunoblotting to see the protein levels of Pol1 and Mcm10-1-aid. Protein extracts prepared from the *mcm10-1-aid* cells were blotted with polyclonal anti-Pol1, anti-aid and monoclonal anti-Pol12 (6D2) antibodies. Asterisk indicates a background protein. Ponceau staining of the membrane is shown as a loading control.

Figure 6

Mcm10 plays an essential role in the initiation but may not play a major role in the elongation in the *mcm10-1-aid* strain. (**a**), (**b**), The YJW50 cells (*mcm10-1-aid, GAL-OsTIR1-9Myc*) and YNK91 cells (*cdc45-aid, GAL-OsTIR1-9Myc*) grown in YPR at 24^{o}C were synchronized in G1 phase in the presence of 7.5 μg/m a-factor for 3 hours, respectively, before being transferred to YPG containing 7.5 μg/ml a-factor for additional 45 min to induce the expression of OsTIR1-9Myc. The culture was split into two for incubation

in the presence (- Mcm10 or - Cdc45) or absence (+ Mcm10 or + Cdc45) of 500 μM IAA (indole-3-acetic acid; auxin) for 1h. The cells were then released into YPG with or without 500 μM IAA, respectively, and withdrawn at indicated time points. (**c**), (**d**), The same cells used in a and b were similarly arrested in G1 phase before being transferred to YPR containing 0.2M HU for 50 min. The arrested cells were transferred to YPG containing 0.2M HU for additional 50 min to induce OsTIR1-9Myc before releasing the cells into fresh medium in the presence or absence of 500 μM IAA. Time course samples were taken at the indicated time points. Arrowheads in c indicate that the cells entered to next G1.

Figure 7

Location of chromosomal loci detected by ChIP assay. Two early origins on chromosome III, *ARS305* and *ARS306*, non-origin region, apart 2kb, 4kb, 6kb, and 9kb from *ARS305*, respectively, and late origin on chromosome V, *ARS501* were examined.

Figure 8

Mcm10 association with early firing origins is detected in S phase in an S-CDK dependent manner. (a, c), Flow cytometric analysis of YJW30 (*MCM10-5FLAG*) and YJW52 (*MCM10-5FLAG, GAL-SIC1ΔNT*). The cells were grown in YPR were synchronized in the G1 phase in the presence of 10 μg/ml α-factor for 3 h. They were subsequently transferred to YPG containing

7.5 μg/ml a-factor and incubated for 1 h before being released into YPG. The released cells were sampled at the indicated time points. (b, d), ChIP analysis of Mcm10-5FLAG. The time course samples of YJW30 and YJW52 (S-CDK OFF) cultured in a and c were processed for ChIP to detect Mcm10-5FLAG at the indicated loci. I performed three PCR reactions for each ChIP sample to obtain an SD.

Figure 9

Mcm10 associates with origins in a Cdc45 dependent manner. (a), Flow cytometric analysis of the YJW65 cells (*MCM10-5FLAG, cdc45-aid, GAL-OsTIR1-9Myc*). The cells pre-cultured in YPR were arrested in the G1 phase in the presence of 10 μg/ml a-factor for 3 h. They were transferred to YPG containing 7.5 μg/ml a-factor and subsequently incubated for 45 min. The culture was split into two for incubation in the presence (- Cdc45) or absence (+ Cdc45) of 500 μM IAA for 1 h. The cells were then released into YPG with or without 500 μM IAA and withdrawn at the indicated time points. (b), ChIP analysis of Mcm10-5FLAG. The cells sampled in a were processed for ChIP to detect Mcm10-5FLAG at the indicated loci. I performed three PCR reactions for each ChIP sample to obtain an SD.

Figure 10

Fork association of Cdc45 and Mcm10. (a), Flow cytometric analysis of the YJW54 cells (*CDC45-18MYC, MCM10-5FLAG*). The cells were cultured as

in Figure 10a and released into YPG containing 0.1 M HU. Time course samples were taken at the indicated time points. The budding index of the cells is presented on the right. (b) and (c), ChIP analysis of Cdc45-18Myc and Mcm10-5FLAG. The cells withdrawn in a were processed for ChIP to detect Cdc45-18Myc and Mcm10-5FLAG at the indicated loci. I performed three PCR reactions for each ChIP sample to obtain an SD.

Figure 11

Cdc45 associates with and stays at origins in the absence of Mcm10 (a), Flow cytometric analysis of the YJW60 cells (*CDC45-5FLAG, mcm10-1-aid, GAL-OsTIR1-9Myc*). The cells initially pre-cultured in YPR were synchronized in the G1 phase in the presence of 10 μg/ml a-factor for 3 h. They were transferred to YPG containing 7.5 μg/ml a-factor and subsequently incubated for 45 min. The culture was split into two to further incubate in the presence (- Mcm10) or absence (+ Mcm10) of 500 μM IAA for 1 h before being released into YPG. Time course samples were taken at the indicated time points. (b), ChIP analysis of Cdc45-FLAG. The cells with drawn in a were processed for ChIP to detect Cdc45-5FLAG at the indicated loci. I performed three PCR reactions for each ChIP sample to obtain an SD.

Figure 12

A stable CMG stays at origins in the absence of Mcm10. (a), Schematic illustration of the cell culture procedure used in c. The YJW184 cells

(*PSF2-5FLAG, MCM4-6HA, mcm10-1-aid, GAL-OsTIR1-9Myc*) pre-cultured in YPR were synchronized in the presence of 10 μg/ml a-factor for 3 h before being cultured in YPG containing 7.5 μg/ml a-factor for 45 min. The culture was split into two to incubate either in the presence (- Mcm10) or absence (+ Mcm10) of 500 μM IAA for 1 h before taking G1 samples. The cells were released into YPG containing 0.2 M HU with or without 500 μM IAA and arrested for 50 min to take S phase samples. (b), The cells cultured in **c** were analyzed by flow cytometry (G1 and + HU). To confirm Mcm10 inactivation functionally, the cells arrested in G1 phase were released into YPG with or without 500 μM IAA and DNA replication was analyzed after 50 min (- HU). Even in the absence of HU, DNA replication was not induced in the cells treated with IAA showing that Mcm10 was depleted efficiently in the cells (- HU, - Mcm10). (c), Immunoblotting to detect Mcm4-6HA and Psf2-FLAG. The YJW184 cells (*MCM4-6HA, PSF2-5FLAG, mcm10-1-aid, GAL-OsTIR1-9Myc*) were grown following the protocol shown in a. Extracts were made from the cells arrested in either G1 or S phase for immunoprecipitation of Psf2-5FLAG. One-twentieth of input extracts relative to FLAG IP was loaded as input. Mcm4-6HA and Psf2-5FLAG were detected using monoclonal anti-HA (12CA5, Roche) and anti-FLAG (M2, Sigma) antibodies, respectively. Arrowhead indicates slow-migrating Mcm4. (d), The IP samples from S phase cells prepared as in c were washed with a buffer containing 150, 300, or 500 mM KOAc, respectively. Proteins were detected as in c. The arrowhead indicates slow-migrating Mcm4. (e), The YJW193 cells (*CDC45-3HA,*

PSF2-5FLAG, mcm10-1-aid, GAL-OsTIR1-9Myc) were grown following the protocol shown in a. Extracts were prepared from S phase cells were washed with a buffer containing 150, 300, or 500 mM NaCl, respectively. Mcm4, Cdc45-3HA and Psf2-5FLAG were detected using anti-Mcm4 (yC-19, Santa Cruz), anti-HA (12CA5, Roche) and anti-FLAG (M2, sigma) antibodies, respectively.

Figure 13

RPA loading is defective without Mcm10. (a), Flow cytometric analysis of the YJW97 cells (*RFA1-5FLAG, mcm10-1-aid, GAL-OsTIR1-9Myc*). The cells were cultured as in Figure 11a. (b), ChIP analysis of Rfa1-5FLAG. The cells withdrawn in a were processed for ChIP to detect Rfa1-5FLAG at the indicated loci. I performed three PCR reactions for each ChIP sample to obtain an SD.

Figure 14

The intra-S phase checkpoint is defective without Mcm10. (a), Schematic illustration of the cell culture procedure used in b and c. YJW50 cells (*mcm10-1-aid, GAL-OsTIR1-9Myc*) or YNK91 cells (*cdc45-aid, GAL-OsTIR1-9Myc*) pre-cultured in YPR were synchronized in the presence of 10 μg/ml a-factor for 3 h before being cultured in YPG containing 7.5 μg/ml a-factor for 45 min. The culture was split into two to incubate either in the presence (- Mcm10) or absence (+ Mcm10) of 500 μM IAA for 1 h. Then, the cells were released into YPG containing 0.2 M HU with or without 500 μM IAA.

Time course samples were taken at the indicated time points. (b, c), Immunoblotting to detect Rad53 in the presence of Mcm10 and Cdc45, or in the absence of Mcm10 or Cdc45. Rad53 was detected using polyclonal anti-Rad53 antibody (yC-19, Santa Cruz).

Figure 15

Pol1 associates with origins before origin unwinding. (a), Flow cytometric analysis of the YJW112 cells (*POL1-5FLAG, mcm10-1-aid, GAL-OsTIR1-9Myc*). The cells were cultured as in Figure 11a. (b), The cells withdrawn in a were processed for ChIP to detect Pol1-5FLAG at the indicated loci. I performed three PCR reactions for each ChIP sample to obtain an SD.

Figure 16

The interaction between Pol1 and CMG in the presence or absence of Mcm10 The same strain used in Figure 12c was grown as in Figure 11a. Extracts were made from the cells arrested in either G1 or S phase for immunoprecipitation of Psf2-5FLAG. One-twentieth of input extracts relative to FLAG IP was loaded as input. Pol1 and Psf2-5FLAG were detected using polyclonal anti-Pol1 and anti-FLAG (M2, Sigma) antibodies, respectively. The IP samples from either G1 or S phase cells were washed with a buffer containing 50 mM KOAc.

Figure 17

The interaction between the Mcm10ΔC60 mutant and CMG components. (a), A schematic illustration showing the Mcm10 protein in budding yeast. The region shown in gray, that is conserved in all eukaryotes, contains the OB-fold/Zn-finger DNA binding motif. Two bipartite NLSs are located in the C-terminus of Mcm10. (**b**), The expression of GFP fused each N- and C-termini truncated mutant of Mcm10. YJW203 *(Δmcm10+pMCM10/URA3+pMCM10-GFP/LEU2)*, YJW205 *(Δmcm10+pMCM10/URA3+pmcm10ΔC60-GFP/LEU2)*, YJW206 *(Δmcm10+pMCM10/URA3+pmcm10ΔC107-GFP/LEU2),* YJW204 (*Δmcm10+pMCM10/URA3+pmcm10ΔN150-GFP/LEU2)* were grown overnight in SC-Trp at 30˚C. Log phased these cells were collected. GFP fused each mutant protein was detected by GFP polyclonal antibody (MBL, code No. 598). (c), Viability of cells expressing N- or C-termini truncated mutant of Mcm10 on 5-FOA containing plates. The same strain used in b were grown overnight in SC-Trp at 30˚C, then spotted on SC-Trp or SC-Trp+5-FOA plates and incubated at 30˚C for 2-4 days. (d), Yeast two hybrid (Y2H) assay to investigate the interaction of Mcm10ΔC60 mutant with CMG components, Polα, Ctf4, and Mcm10, respectively. The strains harbouring bait and prey plasmids were spotted on SC-Trp-Leu (+His), SC-Trp-Leu-His (-His), or SC-Trp-Leu-His+3-AT (-His+3-AT) plates and grown at 30˚C for 2-4 days.

Figure 18

Conserved central region of Mcm10 interacts with Mcm2 and Mcm6. (a), A

schematic illustration shows a divided three regions of Mcm10 to examine the interaction with Mcm2 or Mcm6. (b), The strains contain bait and prey plasmids were spotted and grown on SC-Trp-Leu (+His) or SC-Trp-Leu-His (-His) plates at 30˚C.

Figure 19

The non-MCM domain of Mcm2 and Mcm6 interacts with the central region of Mcm10. (a), A schematic illustration shows a divided fragment of Mcm2 or Mcm6 to test the interaction with the central region of Mcm10. (b), The cells harbouring bait and prey plasmids were spotted and grown on SC-Trp-Leu (+His), SC-Trp-Leu-His (-His), or SC-Trp-Leu-His+3-AT (-His+3-AT) at 30˚C.

Figure 20

A summary and a possible role of Mcm10 in the initiation. (a), In the absence of Mcm10, a stable CMG complex is assembled at origins. However, subsequent translocation of CMG and origin unwinding is severely diminished. Thus, there is a novel step for activating assembled CMG in the presence of Mcm10. Furthermore, Polα might be recruited to origins before origin unwinding. (b), As a one possibility, Mcm10 might open the Mcm2-7 ring by interacting with Mcm2 and Mcm6 to extrude ssDNA from Mcm2-7 ring and promotes CMG activation.

a

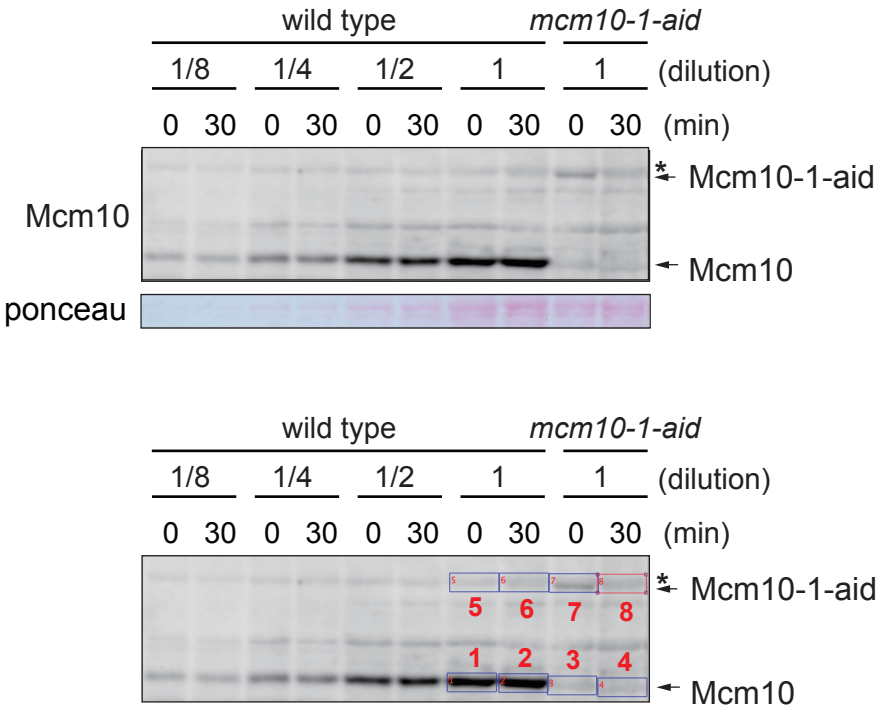

b

	QL/ pixel		BG/ pixel			
Mcm10 in wild type 0'	1. 153.65	–	3. 53.74	=	99.81	**a**
Mcm10-1-aid 0'	7. 62.52	–	5. 49.54	=	14.98	**b**
Mcm10 in wild type 30'	2. 160.58	–	4. 54.31	=	106.27	**c**
Mcm10-1-aid 30'	8. 58.91	–	6. 56.47	=	2.44	**d**

QL: quantitative light absorbance units **BG:** background

Figure S1

Mcm10 depletion efficiency was calculated based on band intensity measured using Multi Gauge software (FUJIFILM). (a) Each band and background area was surrounded by same-pixel sized square (2542 pixel^2). The measured value in each square was shown in (b). The band intensity of Mcm10 or Mcm10-1-aid at each time point was obtained by removing a background signal. The expression level of Mcm10-1-aid vs native Mcm10 at each time point was calculated following formula.

0' Mcm10-1-aid/Mcm10 = **b**/**a** = 0.15 (15%)

30' Mcm10-1-aid/Mcm10 = **d**/**c** = 0.02 (2%)

Figure S1

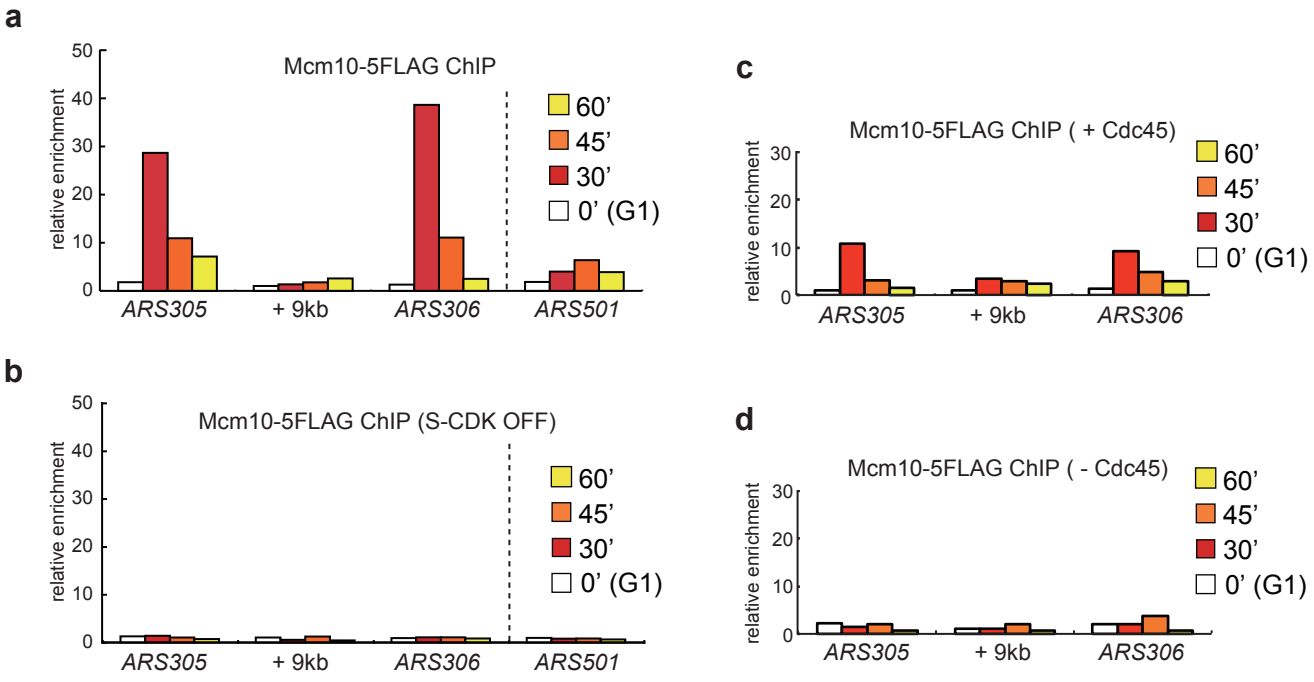

Figure S2

(a) YJW30 cells (*MCM10-5FLAG*) were grown following the protocol shown in Figure 8a. The time course samples were taken at indicated time points and processed for ChIP as described in Materials and methods, except for following points. Each time course sample was processed for immunoprecipitation using anti-FLAG (M2, Sigma) and anti-HA (12CA5, Santa Cruz) monoclonal antibodies, respectively. Cells were disrupted with glass beads using the Micro Smash MS-100 (TOMY SEIKO). DNA prepared from immunoprecipitaed fractions were analyzed by real-time PCR using the Applied Biosystems 7300 Real Time PCR system. The immunoprecipitated samples using anti-HA antibody served as a control. The enrichment of Mcm10 at each tested sequence was calculated according to formula $2^{(Ct\ anti\text{-}HA\ IP - Ct\ anti\text{-}FLAG\ IP)}$. The specific enrichment for each time point were then normalized relative to the background value observed at 0' at the +9kb. The graph shows the average value of twice PCR reactions. (b) YJW52 cells (*MCM10-5FLAG, GAL-SIC1ΔNT*) were cultured as shown in Figure 8c. Samples were processed as in (a). The specific enrichment for each time point were then normalized relative to the background value observed at 0' at the +9kb. The graph shows the average value of twice PCR reactions. (c, d) YJW65 cells (*MCM10-5FLAG, cdc45-aid, GAL-OsTIR1-9Myc*) were grown following the protocol shown in Figure 9a. Samples were processed as in (a). The specific enrichment for each time point were then normalized relative to the background value observed at 0' at the +9kb. The graph shows the average value of twice PCR reactions.

Figure S2

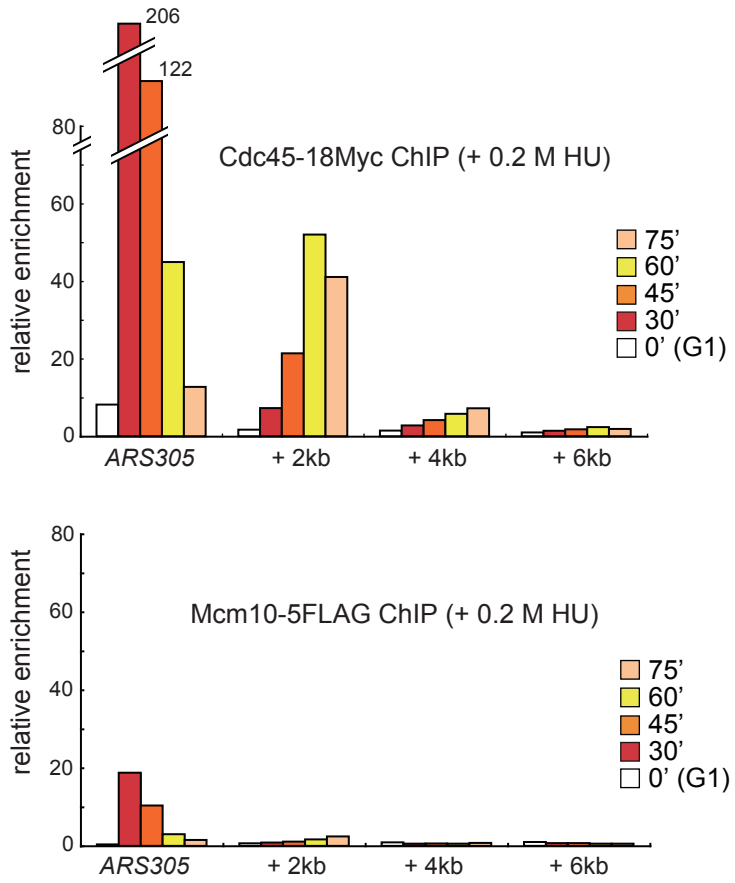

Figure S3

YJW54 cells (*CDC45-18Myc, MCM10-5FLAG*) were cultured as in Figure 10a except for releasing the cells into YPG containing 0.2 M HU. Fork association of Cdc45 and Mcm10 was investigated by same protocol shown in Figure 10. The specific enrichment for each time point were normalized relative to the background value observed at 0' at the +6kb. The graph shows the average value of twice PCR reactions.

Figure S3

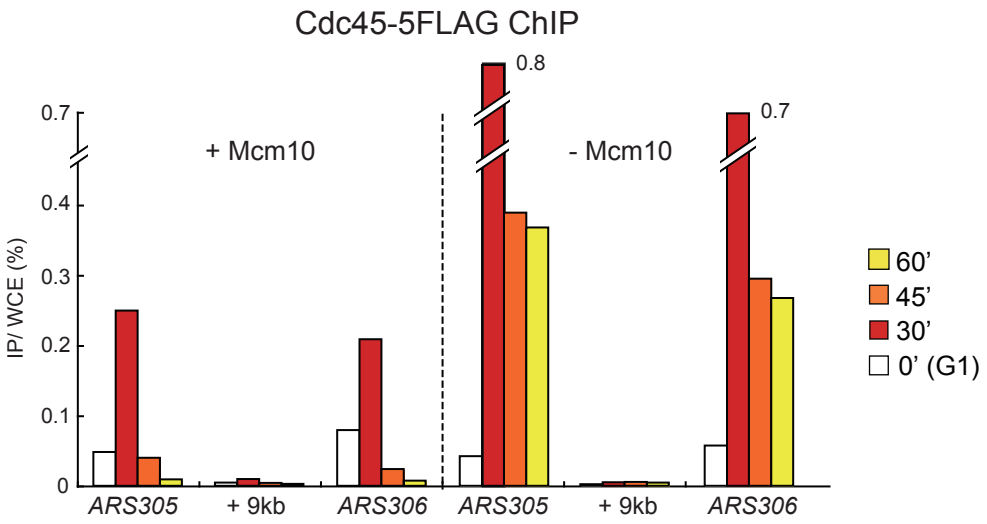

Figure S4

YJW60 cells (*CDC45-5FLAG, mcm10-1-aid, GAL-OsTIR1-9Myc*) were cultured as in Figure 11a. ChIP samples were processed by same protocol shown in Figure 11. The graph shows the average value of twice PCR reactions.

Figure S4

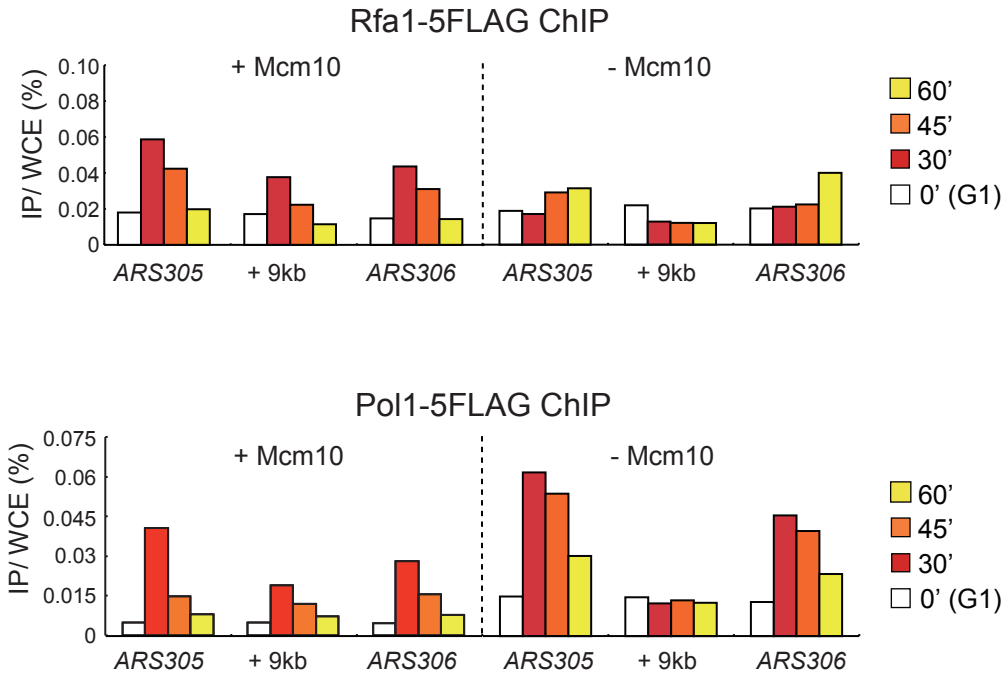

Figure S5

(a) YJW97 cells (*RFA1-5FLAG, mcm10-1-aid, GAL-OsTIR1-9Myc*) were cultured as in Figure 13a. ChIP samples were processed by same protocol shown in Figure 13. The graph shows the average value of twice PCR reactions. (b) YJW112 cells (*POL1-5FLAG, mcm10-1-aid, GAL-OsTIR1-9Myc*) were cultured as in Figure 15a. ChIP samples were processed by same protocol shown in Figure 15. The graph shows the average value of twice PCR reactions.

Figure S5

References

Aparicio, O.M., Weinstein, D.M., and Bell, S.P. (1997). Components and dynamics of DNA replication complexes in *S. cerevisiae*: redistribution of MCM complexes and Cdc45p during S phase. Cell *91*, 59-69.

Bell, S.P., and Stillman, B. (1992). ATP-dependent recognition of eukaryotic origins of DNA replication by a multiprotein complex. Nature *357*, 128-134.

Bochman, M.L., and Schwacha, A. (2009). The Mcm complex: unwinding the mechanism of a replicative helicase. Microbiology and molecular biology reviews : MMBR *73*, 652-683.

Bruck, I., and Kaplan, D. (2009). Dbf4-Cdc7 phosphorylation of Mcm2 is required for cell growth. The Journal of biological chemistry *284*, 28823-28831.

Burich, R., and Lei, M. (2003). Two bipartite NLSs mediate constitutive nuclear localization of Mcm10. Current genetics *44*, 195-201.

Cadoret, J.C., Meisch, F., Hassan-Zadeh, V., Luyten, I., Guillet, C., Duret, L., Quesneville, H., and Prioleau, M.N. (2008). Genome-wide studies highlight indirect links between human replication origins and gene regulation. Proceedings of the National Academy of Sciences of the United States of America *105*, 15837-15842.

Calzada, A., Hodgson, B., Kanemaki, M., Bueno, A., and Labib, K. (2005). Molecular anatomy and regulation of a stable replisome at a paused eukaryotic DNA replication fork. Genes & development *19*, 1905-1919.

Cayrou, C., Coulombe, P., and Mechali, M. (2010). Programming DNA replication origins and chromosome organization. Chromosome research : an international journal on the molecular, supramolecular and evolutionary aspects of chromosome biology *18*, 137-145.

Chattopadhyay, S., and Bielinsky, A.K. (2007). Human Mcm10 regulates the catalytic subunit of DNA polymerase-alpha and prevents DNA damage during replication. Molecular biology of the cell *18*, 4085-4095.

Chong, J.P., Mahbubani, H.M., Khoo, C.Y., and Blow, J.J. (1995). Purification of an MCM-containing complex as a component of the DNA replication licensing system. Nature *375*, 418-421.

Cook, C.R., Kung, G., Peterson, F.C., Volkman, B.F., and Lei, M. (2003). A novel zinc finger is required for Mcm10 homocomplex assembly. The Journal of biological chemistry *278*, 36051-36058.

Costa, A., Ilves, I., Tamberg, N., Petojevic, T., Nogales, E., Botchan, M.R., and Berger, J.M. (2011). The structural basis for MCM2-7 helicase activation by GINS and Cdc45. Nature structural & molecular biology *18*, 471-477.

Delgado, S., Gomez, M., Bird, A., and Antequera, F. (1998). Initiation of DNA replication at CpG islands in mammalian chromosomes. The EMBO journal *17*, 2426-2435.

Dellino, G.I., Cittaro, D., Piccioni, R., Luzi, L., Banfi, S., Segalla, S., Cesaroni, M., Mendoza-Maldonado, R., Giacca, M., and Pelicci, P.G. (2013). Genome-wide mapping of human DNA-replication origins: levels of transcription at ORC1 sites regulate origin selection and replication timing. Genome research *23*, 1-11.

Devault, A., Gueydon, E., and Schwob, E. (2008). Interplay between S-cyclin-dependent kinase and Dbf4-dependent kinase in controlling DNA replication through phosphorylation of yeast Mcm4 N-terminal domain. Molecular biology of the cell *19*, 2267-2277.

Drury, L.S., Perkins, G., and Diffley, J.F.X. (1997). The Cdc4/34/53 pathway targets Cdc6p for proteolysis in budding yeast. EMBO J *16*, 5966-5976.

Dumas, L.B., Lussky, J.P., McFarland, E.J., and Shampay, J. (1982). New

temperature-sensitive mutants of Saccharomyces cerevisiae affecting DNA replication. Molecular & general genetics : MGG *187*, 42-46.

Eisenberg, S., Korza, G., Carson, J., Liachko, I., and Tye, B.K. (2009). Novel DNA binding properties of the Mcm10 protein from Saccharomyces cerevisiae. The Journal of biological chemistry *284*, 25412-25420.

Evrin, C., Clarke, P., Zech, J., Lurz, R., Sun, J., Uhle, S., Li, H., Stillman, B., and Speck, C. (2009). A double-hexameric MCM2-7 complex is loaded onto origin DNA during licensing of eukaryotic DNA replication. Proceedings of the National Academy of Sciences of the United States of America *106*, 20240-20245.

Ferguson, B.M., Brewer, B.J., Reynolds, A.E., and Fangman, W.L. (1991). A yeast origin of replication is activated late in S phase. Cell *65*, 507-515.

Fien, K., Cho, Y.S., Lee, J.K., Raychaudhuri, S., Tappin, I., and Hurwitz, J. (2004). Primer utilization by DNA polymerase alpha-primase is influenced by its interaction with Mcm10p. The Journal of biological chemistry *279*, 16144-16153.

Foiani, M., Liberi, G., Lucchini, G., and Plevani, P. (1995). Cell cycle-dependent phosphorylation and dephosphorylation of the yeast DNA polymerase alpha-primase B subunit. Molecular and cellular biology *15*, 883-891.

Francis, L.I., Randell, J.C., Takara, T.J., Uchima, L., and Bell, S.P. (2009). Incorporation into the prereplicative complex activates the Mcm2-7 helicase for Cdc7-Dbf4 phosphorylation. Genes Dev *23*, 643-654.

Frigola, J., Remus, D., Mehanna, A., and Diffley, J.F. (2013). ATPase-dependent quality control of DNA replication origin licensing. Nature *495*, 339-343.

Fu, Y.V., Yardimci, H., Long, D.T., Ho, T.V., Guainazzi, A., Bermudez, V.P.,

Hurwitz, J., van Oijen, A., Scharer, O.D., and Walter, J.C. (2011). Selective bypass of a lagging strand roadblock by the eukaryotic replicative DNA helicase. Cell *146*, 931-941.

Gambus, A., Jones, R.C., Sanchez-Diaz, A., Kanemaki, M., van Deursen, F., Edmondson, R.D., and Labib, K. (2006). GINS maintains association of Cdc45 with MCM in replisome progression complexes at eukaryotic DNA replication forks. Nature cell biology *8*, 358-366.

Gambus, A., Khoudoli, G.A., Jones, R.C., and Blow, J.J. (2011). MCM2-7 form double hexamers at licensed origins in Xenopus egg extract. The Journal of biological chemistry *286*, 11855-11864.

Gambus, A., van Deursen, F., Polychronopoulos, D., Foltman, M., Jones, R.C., Edmondson, R.D., Calzada, A., and Labib, K. (2009). A key role for Ctf4 in coupling the MCM2-7 helicase to DNA polymerase alpha within the eukaryotic replisome. The EMBO journal *28*, 2992-3004.

Gomez, M., and Antequera, F. (2008). Overreplication of short DNA regions during S phase in human cells. Genes & development *22*, 375-385.

Gregan, J., Lindner, K., Brimage, L., Franklin, R., Namdar, M., Hart, E.A., Aves, S.J., and Kearsey, S.E. (2003). Fission yeast Cdc23/Mcm10 functions after pre-replicative complex formation to promote Cdc45 chromatin binding. Molecular biology of the cell *14*, 3876-3887.

Haworth, J., Alver, R.C., Anderson, M., and Bielinsky, A.K. (2010). Ubc4 and Not4 regulate steady-state levels of DNA polymerase-alpha to promote efficient and accurate DNA replication. Molecular biology of the cell *21*, 3205-3219.

Hayashi, M., Katou, Y., Itoh, T., Tazumi, A., Yamada, Y., Takahashi, T., Nakagawa, T., Shirahige, K., and Masukata, H. (2007). Genome-wide localization of pre-RC sites and identification of replication origins in fission yeast. The EMBO journal *26*, 1327-1339.

Heller, R.C., Kang, S., Lam, W.M., Chen, S., Chan, C.S., and Bell, S.P. (2011). Eukaryotic origin-dependent DNA replication in vitro reveals sequential action of DDK and S-CDK kinases. Cell *146*, 80-91.

Homesley, L., Lei, M., Kawasaki, Y., Sawyer, S., Christensen, T., and Tye, B.K. (2000). Mcm10 and the MCM2-7 complex interact to initiate DNA synthesis and to release replication factors from origins. Genes & development *14*, 913-926.

Ilves, I., Petojevic, T., Pesavento, J.J., and Botchan, M.R. (2010). Activation of the MCM2-7 helicase by association with Cdc45 and GINS proteins. Molecular cell *37*, 247-258.

Ishimi, Y. (1997). A DNA helicase activity is associated with an MCM4, -6, and -7 protein complex. The Journal of biological chemistry *272*, 24508-24513.

Izumi, M., Yanagi, K., Mizuno, T., Yokoi, M., Kawasaki, Y., Moon, K.Y., Hurwitz, J., Yatagai, F., and Hanaoka, F. (2000). The human homolog of Saccharomyces cerevisiae Mcm10 interacts with replication factors and dissociates from nuclease-resistant nuclear structures in G(2) phase. Nucleic Acids Res *28*, 4769-4777.

Kamimura, Y., Tak, Y.S., Sugino, A., and Araki, H. (2001b). Sld3, which interacts with Cdc45 (Sld4), functions for chromosomal DNA replication in Saccharomyces cerevisiae. The EMBO journal *20*, 2097-2107.

Kanemaki, M., and Labib, K. (2006). Distinct roles for Sld3 and GINS during establishment and progression of eukaryotic DNA replication forks. The EMBO journal *25*, 1753-1763.

Kanemaki, M., Sanchez-Diaz, A., Gambus, A., and Labib, K. (2003). Functional proteomic identification of DNA replication proteins by induced proteolysis in vivo. Nature *423*, 720-724.

Kaplan, D.L., Davey, M.J., and O'Donnell, M. (2003). Mcm4,6,7 uses a "pump in ring" mechanism to unwind DNA by steric exclusion and actively translocate along a duplex. The Journal of biological chemistry *278*, 49171-49182.

Karnani, N., and Dutta, A. (2011). The effect of the intra-S-phase checkpoint on origins of replication in human cells. Genes & development *25*, 621-633.

Katou, Y., Kanoh, Y., Bando, M., Noguchi, H., Tanaka, H., Ashikari, T., Sugimoto, K., and Shirahige, K. (2003). S-phase checkpoint proteins Tof1 and Mrc1 form a stable replication-pausing complex. Nature *424*, 1078-1083.

Kawasaki, Y., Hiraga, S., and Sugino, A. (2000). Interactions between Mcm10p and other replication factors are required for proper initiation and elongation of chromosomal DNA replication in Saccharomyces cerevisiae. Genes to cells : devoted to molecular & cellular mechanisms *5*, 975-989.

Klemm, R.D., Austin, R.J., and Bell, S.P. (1997). Coordinate binding of ATP and origin DNA regulates the ATPase activity of the origin recognition complex. Cell *88*, 493-502.

Kubota, Y., Mimura, S., Nishimoto, S., Takisawa, H., and Nojima, H. (1995). Identification of the yeast MCM3-related protein as a component of Xenopus DNA replication licensing factor. Cell *81*, 601-609.

Lee, D.G., Makhov, A.M., Klemm, R.D., Griffith, J.D., and Bell, S.P. (2000). Regulation of origin recognition complex conformation and ATPase activity: differential effects of single-stranded and double-stranded DNA binding. The EMBO journal *19*, 4774-4782.

Lee, J.K., and Hurwitz, J. (2000). Isolation and characterization of various complexes of the minichromosome maintenance proteins of Schizosaccharomyces pombe. The Journal of biological chemistry *275*, 18871-18878.

Liu, C., Wu, R., Zhou, B., Wang, J., Wei, Z., Tye, B.K., Liang, C., and Zhu, G.

(2012). Structural insights into the Cdt1-mediated MCM2-7 chromatin loading. Nucleic acids research *40*, 3208-3217.

Lucchini, G., Brandazza, A., Badaracco, G., Bianchi, M., and Plevani, P. (1985). Identification of the yeast DNA polymerase I gene with antibody probes. Current genetics *10*, 245-252.

Maine, G.T., Surosky, R.T., and Tye, B.K. (1984). Isolation and characterization of the centromere from chromosome V (CEN5) of Saccharomyces cerevisiae. Molecular and cellular biology *4*, 86-91.

Masai, H., Matsumoto, S., You, Z., Yoshizawa-Sugata, N., and Oda, M. (2010). Eukaryotic chromosome DNA replication: where, when, and how? Annual review of biochemistry *79*, 89-130.

Mechali, M. (2010). Eukaryotic DNA replication origins: many choices for appropriate answers. Nature reviews Molecular cell biology *11*, 728-738.

Merchant, A.M., Kawasaki, Y., Chen, Y., Lei, M., and Tye, B.K. (1997). A lesion in the DNA replication initiation factor Mcm10 induces pausing of elongation forks through chromosomal replication origins in Saccharomyces cerevisiae. Molecular and cellular biology *17*, 3261-3271.

Mimura, S., Komata, M., Kishi, T., Shirahige, K., and Kamura, T. (2009). SCF(Dia2) regulates DNA replication forks during S-phase in budding yeast. The EMBO journal *28*, 3693-3705.

Mimura, S., Yamaguchi, T., Ishii, S., Noro, E., Katsura, T., Obuse, C., and Kamura, T. (2010). Cul8/Rtt101 forms a variety of protein complexes that regulate DNA damage response and transcriptional silencing. The Journal of biological chemistry *285*, 9858-9867.

Moyer, S.E., Lewis, P.W., and Botchan, M.R. (2006). Isolation of the Cdc45/Mcm2-7/GINS (CMG) complex, a candidate for the eukaryotic DNA replication fork helicase. Proceedings of the National Academy of Sciences of

the United States of America *103*, 10236-10241.

Muramatsu, S., Hirai, K., Tak, Y.S., Kamimura, Y., and Araki, H. (2010). CDK-dependent complex formation between replication proteins Dpb11, Sld2, Pol (epsilon}, and GINS in budding yeast. Genes & development *24*, 602-612.

Nick McElhinny, S.A., Gordenin, D.A., Stith, C.M., Burgers, P.M., and Kunkel, T.A. (2008). Division of labor at the eukaryotic replication fork. Molecular cell *30*, 137-144.

Nishimura, K., Fukagawa, T., Takisawa, H., Kakimoto, T., and Kanemaki, M. (2009). An auxin-based degron system for the rapid depletion of proteins in nonplant cells. Nature methods *6*, 917-922.

Pacek, M., Tutter, A.V., Kubota, Y., Takisawa, H., and Walter, J.C. (2006). Localization of MCM2-7, Cdc45, and GINS to the site of DNA unwinding during eukaryotic DNA replication. Molecular cell *21*, 581-587.

Pursell, Z.F., Isoz, I., Lundstrom, E.B., Johansson, E., and Kunkel, T.A. (2007). Yeast DNA polymerase epsilon participates in leading-strand DNA replication. Science *317*, 127-130.

Raghuraman, M.K., Winzeler, E.A., Collingwood, D., Hunt, S., Wodicka, L., Conway, A., Lockhart, D.J., Davis, R.W., Brewer, B.J., and Fangman, W.L. (2001). Replication dynamics of the yeast genome. Science *294*, 115-121.

Randell, J.C., Bowers, J.L., Rodriguez, H.K., and Bell, S.P. (2006). Sequential ATP hydrolysis by Cdc6 and ORC directs loading of the Mcm2-7 helicase. Molecular cell *21*, 29-39.

Remus, D., Beuron, F., Tolun, G., Griffith, J.D., Morris, E.P., and Diffley, J.F. (2009). Concerted loading of Mcm2-7 double hexamers around DNA during DNA replication origin licensing. Cell *139*, 719-730.

Ricke, R.M., and Bielinsky, A.K. (2004). Mcm10 regulates the stability and

chromatin association of DNA polymerase-alpha. Mol Cell *16*, 173-185.

Ricke, R.M., and Bielinsky, A.K. (2006). A conserved Hsp10-like domain in Mcm10 is required to stabilize the catalytic subunit of DNA polymerase-alpha in budding yeast. The Journal of biological chemistry *281*, 18414-18425.

Robertson, P.D., Warren, E.M., Zhang, H., Friedman, D.B., Lary, J.W., Cole, J.L., Tutter, A.V., Walter, J.C., Fanning, E., and Eichman, B.F. (2008). Domain architecture and biochemical characterization of vertebrate Mcm10. The Journal of biological chemistry *283*, 3338-3348.

Sawyer, S.L., Cheng, I.H., Chai, W., and Tye, B.K. (2004). Mcm10 and Cdc45 cooperate in origin activation in Saccharomyces cerevisiae. Journal of molecular biology *340*, 195-202.

Sequeira-Mendes, J., Diaz-Uriarte, R., Apedaile, A., Huntley, D., Brockdorff, N., and Gomez, M. (2009). Transcription initiation activity sets replication origin efficiency in mammalian cells. PLoS genetics *5*, e1000446.

Sheu, Y.J., and Stillman, B. (2006). Cdc7-Dbf4 phosphorylates MCM proteins via a docking site-mediated mechanism to promote S phase progression. Molecular cell *24*, 101-113.

Sheu, Y.J., and Stillman, B. (2010). The Dbf4-Cdc7 kinase promotes S phase by alleviating an inhibitory activity in Mcm4. Nature *463*, 113-117.

Solomon, L.R., Massom, L.R., and Jarrett, H.W. (1992). Enzymatic syntheses of DNA-silicas using DNA polymerase. Analytical biochemistry *203*, 58-69.

Speck, C., Chen, Z., Li, H., and Stillman, B. (2005). ATPase-dependent cooperative binding of ORC and Cdc6 to origin DNA. Nature structural & molecular biology *12*, 965-971.

Takenaka, H., Makise, M., Kuwae, W., Takahashi, N., Tsuchiya, T., and Mizushima, T. (2004). ADP-binding to origin recognition complex of

Saccharomyces cerevisiae. Journal of molecular biology *340*, 29-37.

Tanaka, S., and Diffley, J.F. (2002). Interdependent nuclear accumulation of budding yeast Cdt1 and Mcm2-7 during G1 phase. Nature cell biology *4*, 198-207.

Tanaka, S., Nakato, R., Katou, Y., Shirahige, K., and Araki, H. (2011). Origin association of Sld3, Sld7, and Cdc45 proteins is a key step for determination of origin-firing timing. Current biology : CB *21*, 2055-2063.

Tanaka, S., Umemori, T., Hirai, K., Muramatsu, S., Kamimura, Y., and Araki, H. (2007). CDK-dependent phosphorylation of Sld2 and Sld3 initiates DNA replication in budding yeast. Nature *445*, 328-332.

Tanaka, T., and Nasmyth, K. (1998). Association of RPA with chromosomal replication origins requires an Mcm protein, and is regulated by Rad53, and cyclin- and Dbf4-dependent kinases. EMBO J *17*, 5182-5191.

Taylor, M., Moore, K., Murray, J., Aves, S.J., and Price, C. (2011). Mcm10 interacts with Rad4/Cut5(TopBP1) and its association with origins of DNA replication is dependent on Rad4/Cut5(TopBP1). DNA Repair (Amst).

Tercero, J.A., Labib, K., and Diffley, J.F.X. (2000). DNA synthesis at individual replication forks requires the essential initiation factor, Cdc45p. EMBO J *19*, 2082-2093.

van Deursen, F., Sengupta, S., De Piccoli, G., Sanchez-Diaz, A., and Labib, K. (2012). Mcm10 associates with the loaded DNA helicase at replication origins and defines a novel step in its activation. The EMBO journal *31*, 2195-2206.

Warren, E.M., Huang, H., Fanning, E., Chazin, W.J., and Eichman, B.F. (2009). Physical interactions between Mcm10, DNA, and DNA polymerase alpha. The Journal of biological chemistry *284*, 24662-24672.

Warren, E.M., Vaithiyalingam, S., Haworth, J., Greer, B., Bielinsky, A.K.,

Chazin, W.J., and Eichman, B.F. (2008). Structural basis for DNA binding by replication initiator Mcm10. Structure *16*, 1892-1901.

Wei, Z., Liu, C., Wu, X., Xu, N., Zhou, B., Liang, C., and Zhu, G. (2010). Characterization and structure determination of the Cdt1 binding domain of human minichromosome maintenance (Mcm) 6. The Journal of biological chemistry *285*, 12469-12473.

Wohlschlegel, J.A., Dhar, S.K., Prokhorova, T.A., Dutta, A., and Walter, J.C. (2002). Xenopus Mcm10 binds to origins of DNA replication after Mcm2-7 and stimulates origin binding of Cdc45. Molecular cell *9*, 233-240.

Wu, R., Wang, J., and Liang, C. (2012). Cdt1p, through its interaction with Mcm6p, is required for the formation, nuclear accumulation and chromatin loading of the MCM complex. Journal of cell science *125*, 209-219.

Yabuuchi, H., Yamada, Y., Uchida, T., Sunathvanichkul, T., Nakagawa, T., and Masukata, H. (2006). Ordered assembly of Sld3, GINS and Cdc45 is distinctly regulated by DDK and CDK for activation of replication origins. The EMBO journal *25*, 4663-4674.

Yardimci, H., Loveland, A.B., Habuchi, S., van Oijen, A.M., and Walter, J.C. (2010). Uncoupling of sister replisomes during eukaryotic DNA replication. Molecular cell *40*, 834-840.

You, Z., and Masai, H. (2008). Cdt1 forms a complex with the minichromosome maintenance protein (MCM) and activates its helicase activity. The Journal of biological chemistry *283*, 24469-24477.

Zegerman, P., and Diffley, J.F. (2007). Phosphorylation of Sld2 and Sld3 by cyclin-dependent kinases promotes DNA replication in budding yeast. Nature *445*, 281-285.

Zhu, W., Ukomadu, C., Jha, S., Senga, T., Dhar, S.K., Wohlschlegel, J.A., Nutt, L.K., Kornbluth, S., and Dutta, A. (2007). Mcm10 and And-1/CTF4 recruit DNA

polymerase alpha to chromatin for initiation of DNA replication. Genes & development *21*, 2288-2299.

Zou, L., and Elledge, S.J. (2003). Sensing DNA damage through ATRIP recognition of RPA-ssDNA complexes. Science *300*, 1542-1548.

Zou, L., and Stillman, B. (1998). Formation of a preinitiation complex by S-phase cyclin CDK-dependent loading of Cdc45p onto chromatin. Science *280*, 593-596.

Acknowledgments

I am great thank to Prof. Haruhiko Takisawa (Osaka University, Japan) and Dr. Masato Kanemaki (National Institute of Genetics, Japan) for giving me an opportunity to do this project and write this thesis. Without their supervision, advice, and encouragement, I would not be where I am now.

I also thank to these people for providing me a material and opportunity to use experimental instruments for carrying out this project.

Prof. Hiroyuki Araki (National Institute of Genetics)
for anti-Mcm10 polyclonal antibody
Dr. Karim Labib (Cancer Research UK, UK)
for anti-Pol1 and -Ctf4 polyclonal antibodies
Prof. Marco Foiani (University of Milan, Italy) and Dr. Satoru Mimura (Osaka University)
for anti-Pol12 monoclonal antibody
Ms. Yoshie Nakajima and Dr. Satoru Mimura (Osaka University)
for yeast two-hybrid construct and strains
Araki Lab (National Institute of Genetics)
for kindly providing an opportunity to use some experimental instruments
Lab members in Kanemaki lab and Takisawa lab
for valuable discussion and warm their support

Finally, I would like to thank to my family, Susumu, Etsuko, Itaru, Misae, and Joko, for their warm support.

George Watase April, 2013